

A New Class of Efficient and Robust Energy Stable Schemes for Gradient Flows*

Jie Shen^{†‡}
Jie Xu[‡]
Jiang Yang[§]

Abstract. We propose a new numerical technique to deal with nonlinear terms in gradient flows. By introducing a scalar auxiliary variable (SAV), we construct efficient and robust energy stable schemes for a large class of gradient flows. The SAV approach is not restricted to specific forms of the nonlinear part of the free energy and only requires solving *decoupled* linear equations with *constant coefficients*. We use this technique to deal with several challenging applications which cannot be easily handled by existing approaches, and we present convincing numerical results to show that our schemes are not only much more efficient and easy to implement, but can also better capture the physical properties in these models. Based on this SAV approach, we can construct unconditionally second-order energy stable schemes, and we can easily construct even third- or fourth-order BDF schemes which, although not unconditionally stable, are very robust in practice. In particular, when coupled with an adaptive time stepping strategy, the SAV approach can be extremely efficient and accurate.

Key words. gradient flows, energy stability, Allen–Cahn and Cahn–Hilliard equations, phase field models, nonlocal models

AMS subject classifications. 65M12, 35K20, 35K35, 35K55, 65Z05

DOI. 10.1137/17M1150153

Contents

1	Introduction	475
2	SAV Approach for Constructing Energy Stable Schemes	478
2.1	Gradient Flows of a Single Function	478
2.2	Gradient Flows of Multiple Functions	482
2.3	Full Discretization	484
3	Numerical Validation	484

*Received by the editors October 2, 2017; accepted for publication (in revised form) January 10, 2018; published electronically August 7, 2019.

<https://doi.org/10.1137/17M1150153>

Funding: This work was partially supported by NSFC grants 91630204 and 51661135011, NSF grants DMS-1620262 and DMS-1720442, and AFOSR grant FA9550-16-1-0102.

[†]Fujian Provincial Key Laboratory of Mathematical Modeling and High-Performance Scientific Computing and School of Mathematical Sciences, Xiamen University, Xiamen 361005, China.

[‡]Department of Mathematics, Purdue University, West Lafayette, IN 47907 (shen7@purdue.edu, xu924@purdue.edu).

[§]Department of Mathematics, Southern University of Science and Technology, Shenzhen, Guangdong 518000, China (yangj7@sustc.edu.cn).

3.1	Allen–Cahn, Cahn–Hilliard, and Fractional Cahn–Hilliard Equations	485
3.2	Phase Field Crystals	488
4	Higher-Order SAV Schemes and Adaptive Time Stepping	491
4.1	Higher-Order SAV Schemes	492
4.2	Adaptive Time Stepping	494
5	Various Applications of the SAV Approach	496
5.1	Gradient Flows with Nonlocal Free Energy	496
5.2	Molecular Beam Epitaxial (MBE) without Slope Selection	497
5.3	Q-Tensor Model for Rod-Like Liquid Crystals	498
6	Conclusion	501
	References	503

I. Introduction. Gradient flows are dynamics driven by a free energy. Many physical problems can be modeled by PDEs taking the form of gradient flows, which are often derived from the second law of thermodynamics. Examples of these problems include interface dynamics [4, 42, 46, 52, 53, 76], crystallization [27, 26, 28], thin films [38, 58], polymers [56, 34, 35, 36], and liquid crystals [49, 23, 47, 48, 33, 32, 60, 75].

A gradient flow is determined by not only the driving free energy, but also the dissipation mechanism. Given a free energy functional $\mathcal{E}[\phi(\boldsymbol{x})]$ bounded from below, denote its variational derivative as $\mu = \delta\mathcal{E}/\delta\phi$. The general form of the gradient flow can be written as

$$(1.1) \quad \frac{\partial\phi}{\partial t} = \mathcal{G}\mu,$$

supplemented with suitable boundary conditions. To simplify the presentation, we assume throughout the paper that the boundary conditions are chosen such that all boundary terms will vanish when integration by parts is performed. This is true with periodic boundary conditions or homogeneous Neumann boundary conditions.

In the above, a nonpositive symmetric operator \mathcal{G} gives the dissipation mechanism. Commonly adopted dissipation mechanisms include L^2 gradient flow where $\mathcal{G} = -I$, H^{-1} gradient flow where $\mathcal{G} = \Delta$, or more generally nonlocal $H^{-\alpha}$ gradient flow where $\mathcal{G} = -(-\Delta)^\alpha$ ($0 < \alpha < 1$) (cf. [1]). For more complicated dissipation mechanisms, \mathcal{G} may be nonlinear and may depend on ϕ . An example of this is the Wasserstein gradient flow for $\phi > 0$, where $\mathcal{G}\mu = \nabla \cdot (\phi\nabla\mu)$ (cf. [23, 44]). As long as \mathcal{G} is nonpositive, the free energy is nonincreasing,

$$(1.2) \quad \frac{d\mathcal{E}[\phi]}{dt} = \frac{\delta\mathcal{E}}{\delta\phi} \cdot \frac{\partial\phi}{\partial t} = (\mu, \mathcal{G}\mu) \leq 0,$$

where $(\phi, \psi) = \int_{\Omega} \phi\psi d\boldsymbol{x}$. In this paper, we will focus on the case where \mathcal{G} is nonpositive, linear, and independent of ϕ .

Although gradient flows take various forms, from the numerical perspective a scheme is generally evaluated by considering the following aspects:

- (i) whether the scheme keeps the energy dissipation;
- (ii) whether the scheme is convergent, and if error bounds can be established;

- (iii) its efficiency;
- (iv) whether the scheme is easy to implement.

Among these the first aspect is particularly important and is crucial to eliminate numerical results that are not physical. Often, if this is not thoroughly considered when constructing the scheme, it may require a time step that is extremely small to maintain the energy dissipation.

Usually, the free energy functional contains a quadratic term, which we write explicitly as

$$(1.3) \quad \mathcal{E}[\phi] = \frac{1}{2}(\phi, \mathcal{L}\phi) + \mathcal{E}_1[\phi],$$

where \mathcal{L} is a symmetric nonnegative linear operator (also independent of ϕ), and $\mathcal{E}_1[\phi]$ are nonlinear but usually with only derivatives of lower order than \mathcal{L} . To obtain an energy dissipative scheme, the linear term is usually treated implicitly in some manner, while different approaches have to be used for the nonlinear terms. In the next few paragraphs, we briefly review the existing approaches for dealing with the nonlinear terms.

The first approach is the convex splitting method, which was perhaps first introduced in [29] but popularized by [31, 8, 9]. If we can express the free energy as the difference of two convex functionals, namely, $\mathcal{E} = \mathcal{E}_c - \mathcal{E}_e$, where both \mathcal{E}_c and \mathcal{E}_e are convex about ϕ , then a simple convex splitting scheme reads

$$(1.4) \quad \frac{\phi^{n+1} - \phi^n}{\Delta t} = \mathcal{G} \left(\frac{\delta \mathcal{E}_c}{\delta \phi}[\phi^{n+1}] - \frac{\delta \mathcal{E}_e}{\delta \phi}[\phi^n] \right).$$

Using the property of the convex functional

$$\mathcal{E}_c[\phi_2] - \mathcal{E}_c[\phi_1] \geq \frac{\delta \mathcal{E}_c}{\delta \phi}[\phi_1](\phi_2 - \phi_1),$$

and multiplying (1.4) with $(\delta \mathcal{E}_c / \delta \phi)[\phi^{n+1}] - (\delta \mathcal{E}_e / \delta \phi)[\phi^n]$, it is easy to check that the scheme satisfies the discrete energy law $\mathcal{E}[\phi^{n+1}] \leq \mathcal{E}[\phi^n]$ unconditionally. Because the implicit part $\delta \mathcal{E}_c / \delta \phi$ is usually nonlinear about ϕ , we need to solve nonlinear equations at each time step, which can be expensive. The scheme (1.4) is only first order. While it is possible to construct second-order convex splitting schemes for certain situations on a case-by-case basis (see, for instance, [65, 10, 72]), a general formulation of second-order convex splitting schemes is not available.

The second approach is the so-called stabilization method, which treats the nonlinear terms explicitly and adds a stabilization term to avoid strict time step constraints [79, 69]. More precisely, if we can find a simple linear operator $\tilde{\mathcal{L}}$ such that both $\tilde{\mathcal{L}}$ and $\tilde{\mathcal{L}} - (\delta^2 \mathcal{E}_1 / \delta \phi^2)[\phi]$ are positive, then we may choose a particular convex splitting,

$$\mathcal{E}_c = \frac{1}{2}(\phi, \mathcal{L}\phi) + \frac{1}{2}(\phi, \tilde{\mathcal{L}}\phi), \quad \mathcal{E}_e = \frac{1}{2}(\phi, \tilde{\mathcal{L}}\phi) - \mathcal{E}_1[\phi],$$

which leads to the following unconditionally energy stable scheme:

$$(1.5) \quad \frac{\phi^{n+1} - \phi^n}{\Delta t} = \mathcal{G} \left(\mathcal{L}\phi^{n+1} + \frac{\delta \mathcal{E}_1}{\delta \phi}[\phi^n] + \tilde{\mathcal{L}}(\phi^{n+1} - \phi^n) \right).$$

Hence, the stabilization method is in fact a special class of convex splitting method. A common choice of $\tilde{\mathcal{L}}$ is

$$\tilde{\mathcal{L}} = a_0 + a_1(-\Delta) + a_2(-\Delta)^2 + \dots.$$

The advantage of the stabilization method is that when the dissipation operator \mathcal{G} is also linear, we only need to solve a linear system like $(1 - \Delta t \mathcal{G}(\mathcal{L} + \tilde{\mathcal{L}}))\phi^{n+1} = b^n$ at each time step. However, it is not always the case that $\tilde{\mathcal{L}}$ can be found. The stabilization method can be extended to second-order schemes, but in general it cannot be unconditionally energy stable; see, however, the recent work in [51]. On the other hand, a related method is the exponential time differencing (ETD) approach in which the operator $\tilde{\mathcal{L}}$ is integrated exactly (see, for instance, [45] for an example on related applications).

The third approach is the method of invariant energy quadratization (IEQ), which was proposed very recently in [74, 77]. This method is a generalization of the method of Lagrange multipliers or of auxiliary variables, originally proposed in [6, 41]. In this approach, \mathcal{E}_1 is assumed to take the form $\mathcal{E}_1[\phi] = \int_{\Omega} g(\phi) d\mathbf{x}$, where $g \in C^1(\mathbb{R})$ and $g(s) > -C_0 \forall s \in \mathbb{R}$ for some $C_0 > 0$. The IEQ also allows us to deal with $g = g(\phi, \nabla\phi)$, where $g \in C^1(\mathbb{R}^4)$ and $g > -C_0$, or it involves higher-order derivatives. For simplicity, we only present the case where $g = g(\phi)$. One then introduces an auxiliary variable $q = \sqrt{g + C_0}$ and transforms (1.1) into an equivalent system,

$$(1.6a) \quad \frac{\partial \phi}{\partial t} = \mathcal{G} \left(\mathcal{L}\phi + \frac{q}{\sqrt{g(\phi) + C_0}} g'(\phi) \right),$$

$$(1.6b) \quad \frac{\partial q}{\partial t} = \frac{g'(\phi)}{2\sqrt{g(\phi) + C_0}} \frac{\partial \phi}{\partial t}.$$

Using the fact that $\mathcal{E}_1[\phi] = \int_{\Omega} q^2 d\mathbf{x}$ is convex about q , we can easily construct simple and linear energy stable schemes. For instance, a first-order scheme is given by

$$(1.7a) \quad \frac{\phi^{n+1} - \phi^n}{\Delta t} = \mathcal{G}\mu^{n+1},$$

$$(1.7b) \quad \mu^{n+1} = \mathcal{L}\phi^{n+1} + \frac{q^{n+1}}{\sqrt{g(\phi^n) + C_0}} g'(\phi^n),$$

$$(1.7c) \quad \frac{q^{n+1} - q^n}{\Delta t} = \frac{g'(\phi^n)}{2\sqrt{g(\phi^n) + C_0}} \frac{\phi^{n+1} - \phi^n}{\Delta t}.$$

One can easily show that the above scheme is unconditionally energy stable. Furthermore, eliminating q^{n+1} and μ^{n+1} , we obtain a linear system for ϕ^{n+1} in the following form:

$$(1.8) \quad \left(\frac{1}{\Delta t} - \mathcal{G}\mathcal{L} - \mathcal{G} \frac{(g'(\phi^n))^2}{2g(\phi^n)} \right) \phi^{n+1} = b^n.$$

Similarly, one can also construct unconditionally energy stable second-order schemes. The IEQ approach is remarkable as it allows us to construct linear, unconditionally stable, and second-order unconditionally energy stable schemes for a large class of gradient flows. However, it still suffers from the following drawbacks:

- Although one only needs to solve a linear system at each time step, the linear system usually involves variable coefficients which change at each time step.
- For gradient flows with multiple components, the IEQ approach will lead to coupled systems with variable coefficients.
- It requires that \mathcal{E}_1 has the form $\int_{\Omega} g(\phi) d\mathbf{x}$, or more generally $\int_{\Omega} g(\phi, \nabla\phi, \dots, \nabla^m\phi) d\mathbf{x}$, where the energy density g is bounded from below. However, in some cases, \mathcal{E}_1 does not take such a form. Even if one can find such a g , it might be unbounded from below while $\mathcal{E}_1[\phi]$ is bounded from below.

In [68], we introduced the so-called scalar auxiliary variable (SAV) approach, which inherits all the advantages of the IEQ approach but also overcomes most of its shortcomings. More precisely, using the Cahn–Hilliard equation and a system of Cahn–Hilliard equations as examples, we showed that the SAV approach has the following advantages:

- (i) For single-component gradient flows, at each time step it leads to linear equations with constant coefficients, so it is remarkably easy to implement.
- (ii) For multicomponent gradient flows, at each time step it leads to decoupled linear equations with constant coefficients, one for each component.

The main goals of this paper are (i) to expand the SAV approach to a more general setting and apply it to several challenging applications, such as nonlocal phase field crystals, a molecular beam epitaxial without slope section, and a Q-tensor model for liquid crystals; (ii) to show numerically that, besides their simplicity and efficiency, the novel schemes present better accuracy compared with other schemes for many equations; and (iii) to validate the effectiveness and robustness of the SAV approach coupled with high-order BDF schemes and adaptive time stepping.

We emphasize that the schemes are formulated in a general form that is applicable to a large class of gradient flows. We also suggest some criteria on the choice of \mathcal{L} and \mathcal{E}_1 , which is useful when attempting to construct numerical schemes for particular gradient flows.

The rest of the paper is organized as follows. In section 2, we describe the construction of SAV schemes for gradient flows in a general form. In section 3, we present several numerical examples to validate the SAV approach. In section 4, we describe how to construct higher-order SAV schemes and how to implement adaptive time stepping. We then apply the SAV approach to construct second-order unconditionally stable, decoupled linear schemes for several challenging situations in section 5, followed by some concluding remarks in section 6.

2. SAV Approach for Constructing Energy Stable Schemes. In this section, we formulate the SAV approach introduced in [68] for a class of general gradient flows.

2.1. Gradient Flows of a Single Function. We consider the gradient flow (1.1) with free energy in the form of (1.3) such that $\mathcal{E}_1[\phi]$ is bounded from below. Without loss of generality, we assume that $\mathcal{E}_1[\phi] \geq C_0 > 0$, otherwise we may add a constant to \mathcal{E}_1 without altering the gradient flow. We introduce an SAV $r = \sqrt{\mathcal{E}_1}$ and rewrite the gradient flow (1.1) as

$$(2.1a) \quad \frac{\partial \phi}{\partial t} = \mathcal{G}\mu,$$

$$(2.1b) \quad \mu = \mathcal{L}\phi + \frac{r}{\sqrt{\mathcal{E}_1[\phi]}}U[\phi],$$

$$(2.1c) \quad \frac{dr}{dt} = \frac{1}{2\sqrt{\mathcal{E}_1[\phi]}} \int_{\Omega} U[\phi] \frac{\partial \phi}{\partial t} d\mathbf{x},$$

where

$$(2.2) \quad U[\phi] = \frac{\delta \mathcal{E}_1}{\delta \phi}.$$

Taking the inner products of the above with μ , $\frac{\partial \phi}{\partial t}$, and $2r$, respectively, we obtain the following energy dissipation law for (2.1):

$$(2.3) \quad \frac{d\mathcal{E}[\phi(t)]}{dt} = \frac{d}{dt} \left[\frac{1}{2}(\phi, \mathcal{L}\phi) + r^2 \right] = (\mu, \mathcal{G}\mu).$$

Note that this equivalent system (2.1) is similar to the system (1.6a) and (1.6b) in the IEQ approach, except that an SAV r is introduced instead of a function $q(\phi)$. To illustrate the advantage of SAV over IEQ, we start with the first-order scheme

$$(2.4a) \quad \frac{\phi^{n+1} - \phi^n}{\Delta t} = \mathcal{G}\mu^{n+1},$$

$$(2.4b) \quad \mu^{n+1} = \mathcal{L}\phi^{n+1} + \frac{r^{n+1}}{\sqrt{\mathcal{E}_1[\phi^n]}} U[\phi^n],$$

$$(2.4c) \quad \frac{r^{n+1} - r^n}{\Delta t} = \frac{1}{2\sqrt{\mathcal{E}_1[\phi^n]}} \int_{\Omega} U[\phi^n] \frac{\phi^{n+1} - \phi^n}{\Delta t} d\mathbf{x}.$$

Multiplying the three equations with μ^{n+1} , $(\phi^{n+1} - \phi^n)/\Delta t$, and $2r^{n+1}$, integrating the first two equations, and adding them together, we obtain the discrete energy law

$$\begin{aligned} & \frac{1}{\Delta t} \left[\tilde{\mathcal{E}}[\phi^{n+1}, r^{n+1}] - \tilde{\mathcal{E}}[\phi^n, r^n] \right] \\ & + \frac{1}{\Delta t} \left[\frac{1}{2}(\phi^{n+1} - \phi^n, \mathcal{L}(\phi^{n+1} - \phi^n)) + (r^{n+1} - r^n)^2 \right] = (\mu^{n+1}, \mathcal{G}\mu^{n+1}), \end{aligned}$$

where we have defined the modified energy

$$(2.5) \quad \tilde{\mathcal{E}}[\eta, s] = \frac{1}{2}(\eta, \mathcal{L}\eta) + s^2.$$

Thus, the scheme is unconditionally energy stable with the modified energy. Note that, while $r = \sqrt{\mathcal{E}_1[\phi]}$, we do not have $r^n = \sqrt{\mathcal{E}_1[\phi^n]}$, so the modified energy $\tilde{\mathcal{E}}[\phi^n, r^n]$ is different from the original energy $\mathcal{E}[\phi^n]$.

REMARK 2.1. Notice that the SAV scheme (2.4) is unconditionally energy stable (with a modified energy) for arbitrary energy splitting in (1.3) as long as \mathcal{E}_1 is bounded from below. One might wonder, why not take $\mathcal{L} = 0$? Then the scheme (2.4) would be totally explicit, i.e., without the need to solve any equation, but unconditionally energy stable (with a modified energy $\tilde{\mathcal{E}}[\eta, s] = \frac{1}{2}(\eta, \mathcal{L}\eta) + s^2 = s^2$)! However, energy stability alone is not sufficient for convergence. Such a scheme could not produce meaningful results, since the modified energy (2.5) reduces to s^2 which cannot control any oscillation due to derivative terms. Hence, it is necessary that \mathcal{L} contains enough dissipative terms (with at least linearized highest derivative terms).

An important fact is that the SAV scheme (2.4) is easy to implement. To this end, we write (2.4) in the form

$$(2.6) \quad \begin{pmatrix} \frac{1}{\Delta t}I & -\mathcal{G} & 0 \\ -\mathcal{L} & I & * \\ * & 0 & \frac{1}{\Delta t}I \end{pmatrix} \begin{pmatrix} \phi^{n+1} \\ \mu^{n+1} \\ r^{n+1} \end{pmatrix} = \bar{b}^n,$$

where \bar{b}^n is the vector with known quantities, and $*$ is some vector with variable coefficients. Hence, we can solve r^{n+1} with a block Gaussian elimination, which requires solving a system with constant coefficients of the form

$$(2.7) \quad \begin{pmatrix} \frac{1}{\Delta t}I & -\mathcal{G} \\ -\mathcal{L} & I \end{pmatrix} \begin{pmatrix} \phi \\ \mu \end{pmatrix} = \bar{b}.$$

Once r^{n+1} is known, we can obtain (ϕ^{n+1}, μ^{n+1}) by solving one more equation in the above form.

For the readers' convenience, we give below another explicit procedure for solving (2.4). Substituting (2.4b) and (2.4c) into (2.4a), we obtain

$$(2.8) \quad \frac{\phi^{n+1} - \phi^n}{\Delta t} = \mathcal{G} \left[\mathcal{L}\phi^{n+1} + \frac{U[\phi^n]}{\sqrt{\mathcal{E}_1[\phi^n]}} \left(r^n + \int_{\Omega} \frac{U[\phi^n]}{2\sqrt{\mathcal{E}_1[\phi^n]}} (\phi^{n+1} - \phi^n) d\mathbf{x} \right) \right].$$

Denote

$$b^n = U[\phi^n] / \sqrt{\mathcal{E}_1[\phi^n]}.$$

Then the above equation can be written as

$$(2.9) \quad (I - \Delta t \mathcal{G} \mathcal{L}) \phi^{n+1} - \frac{\Delta t}{2} \mathcal{G} b^n (b^n, \phi^{n+1}) = \phi^n + \Delta t r^n \mathcal{G} b^n - \frac{\Delta t}{2} (b^n, \phi^n) \mathcal{G} b^n.$$

Denote the right-hand side of (2.9) by c^n . Multiplying (2.9) with $(I - \Delta t \mathcal{G} \mathcal{L})^{-1}$, then taking the inner product with b^n , we obtain

$$(2.10) \quad (b^n, \phi^{n+1}) + \frac{\Delta t}{2} \gamma^n (b^n, \phi^{n+1}) = (b^n, (I - \Delta t \mathcal{G} \mathcal{L})^{-1} c^n),$$

where $\gamma^n = -(b^n, (I - \Delta t \mathcal{G} \mathcal{L})^{-1} \mathcal{G} b^n) = (b^n, (-\mathcal{G}^{-1} + \Delta t \mathcal{L})^{-1} b^n) > 0$, if we assume that \mathcal{G} is negative definite and \mathcal{L} is nonnegative. Hence,

$$(2.11) \quad (b^n, \phi^{n+1}) = \frac{(b^n, (I - \Delta t \mathcal{G} \mathcal{L})^{-1} c^n)}{1 + \Delta t \gamma^n / 2}.$$

To summarize, we implement (2.4) as follows:

- (i) Compute b^n and c^n (the right-hand side of (2.9)).
- (ii) Compute (b^n, ϕ^{n+1}) from (2.11).
- (iii) Compute ϕ^{n+1} from (2.9).

Note that in steps (ii) and (iii) of the above procedure, we only need to solve, twice, a linear equation with constant coefficients of the form

$$(2.12) \quad (I - \Delta t \mathcal{G} \mathcal{L}) \bar{x} = \bar{b},$$

which is exactly (2.7) with μ eliminated. Therefore, the above procedure is extremely efficient. In particular, if $\mathcal{L} = -\Delta$ and $\mathcal{G} = -1$ or $-\Delta$, with a tensor-product domain Ω , fast solvers are available. In contrast, convex splitting schemes usually require solving a nonlinear system, while the IEQ scheme requires solving (1.8), which involves variable coefficients.

A main advantage of the SAV approach (as well as the IEQ approach) is that linear second- or even higher-order energy stable schemes can be easily constructed. We start with a semi-implicit second-order scheme based on Crank–Nicolson, which we denote as SAV/CN:

$$(2.13a) \quad \frac{\phi^{n+1} - \phi^n}{\Delta t} = \mathcal{G} \mu^{n+1/2},$$

$$(2.13b) \quad \mu^{n+1/2} = \mathcal{L} \frac{1}{2} (\phi^{n+1} + \phi^n) + \frac{r^{n+1} + r^n}{2\sqrt{\mathcal{E}_1[\bar{\phi}^{n+1/2}]}} U[\bar{\phi}^{n+1/2}],$$

$$(2.13c) \quad r^{n+1} - r^n = \int_{\Omega} \frac{U[\bar{\phi}^{n+1/2}]}{2\sqrt{\mathcal{E}_1[\bar{\phi}^{n+1/2}]}} (\phi^{n+1} - \phi^n) d\mathbf{x}.$$

In the above, $\bar{\phi}^{n+1/2}$ can be any explicit approximation of $\phi(t^{n+1/2})$ with an error of $O(\Delta t^2)$. For instance, we may let

$$(2.14) \quad \bar{\phi}^{n+1/2} = \frac{1}{2}(3\phi^n - \phi^{n-1})$$

be the extrapolation, or we can use a simple first-order scheme to obtain it, such as the semi-implicit scheme

$$(2.15) \quad \frac{\bar{\phi}^{n+1/2} - \phi^n}{\Delta t/2} = \mathcal{G} \left(\mathcal{L}\bar{\phi}^{n+1/2} + U[\phi^n] \right),$$

which has a local truncation error of $O(\Delta t^2)$.

Just as in the first-order scheme, one can eliminate μ^{n+1} and r^{n+1} from the second-order schemes (2.13) to obtain a linear equation for ϕ similar to (2.9), which can be solved using the Sherman–Morrison–Woodbury formula (2.26) that only involves two linear equations with constant coefficients of the form (2.12).

Regardless of how we obtain $\bar{\phi}^{n+1/2}$, multiplying the three equations with $\mu^{n+1/2}$, $(\phi^{n+1} - \phi^n)/\Delta t$, and $(r^{n+1} + r^n)/\Delta t$, we derive the following theorem.

THEOREM 2.1. *The scheme (2.13) is second-order accurate and unconditionally energy stable in the sense that*

$$\frac{1}{\Delta t} \left(\tilde{\mathcal{E}}[\phi^{n+1}, r^{n+1}] - \tilde{\mathcal{E}}[\phi^n, r^n] \right) = (\mu^{n+1/2}, \mathcal{G}\mu^{n+1/2}),$$

where $\tilde{\mathcal{E}}$ is the modified energy defined in (2.5), and one can obtain $(\phi^{n+1}, \mu^{n+1}, r^{n+1})$ by solving two linear equations with constant coefficients of the form (2.12).

We can also construct a semi-implicit second-order scheme based on the BDF formula, which we denote as SAV/BDF:

$$(2.16a) \quad \frac{3\phi^{n+1} - 4\phi^n + \phi^{n-1}}{2\Delta t} = \mathcal{G}\mu^{n+1},$$

$$(2.16b) \quad \mu^{n+1} = \mathcal{L}\phi^{n+1} + \frac{r^{n+1}}{\sqrt{\mathcal{E}_1[\bar{\phi}^{n+1}]}} U[\bar{\phi}^{n+1}],$$

$$(2.16c) \quad 3r^{n+1} - 4r^n + r^{n-1} = \int_{\Omega} \frac{U[\bar{\phi}^{n+1}]}{2\sqrt{\mathcal{E}_1[\bar{\phi}^{n+1}]}} (3\phi^{n+1} - 4\phi^n + \phi^{n-1}) d\mathbf{x}.$$

Here, $\bar{\phi}^{n+1}$ can be any explicit approximation of $\phi(t^{n+1})$ with an error of $O(\Delta t^2)$. Multiplying the three equations with μ^{n+1} , $(3\phi^{n+1} - 4\phi^n + \phi^{n-1})/\Delta t$, and $r^{n+1}/\Delta t$, integrating the first two equations, and using the identity

$$(2.17) \quad \begin{aligned} 2(a^{k+1}, 3a^{k+1} - 4a^k + a^{k-1}) &= |a^{k+1}|^2 + |2a^{k+1} - a^k|^2 + |a^{k+1} - 2a^k + a^{k-1}|^2 \\ &\quad - |a^k|^2 - |2a^k - a^{k-1}|^2, \end{aligned}$$

we obtain the following theorem.

THEOREM 2.2. *The scheme (2.16) is second-order accurate and unconditionally energy stable in the sense that*

$$\begin{aligned} & \frac{1}{\Delta t} \left\{ \tilde{\mathcal{E}}[(\phi^{n+1}, r^{n+1}), (\phi^n, r^n)] - \tilde{\mathcal{E}}[(\phi^n, r^n), (\phi^{n-1}, r^{n-1})] \right\} \\ & + \frac{1}{\Delta t} \left\{ \frac{1}{4} (\phi^{n+1} - 2\phi^n + \phi^{n-1}, \mathcal{L}(\phi^{n+1} - 2\phi^n + \phi^{n-1})) \right. \\ & \left. + \frac{1}{2} (r^{n+1} - 2r^n + r^{n-1})^2 \right\} = (\mu^{n+1}, \mathcal{G}\mu^{n+1}), \end{aligned}$$

where the modified discrete energy is defined as

$$\begin{aligned} \tilde{\mathcal{E}}[(\phi^{n+1}, r^{n+1}), (\phi^n, r^n)] &= \frac{1}{4} \left((\phi^{n+1}, \mathcal{L}\phi^{n+1}) + (2\phi^{n+1} - \phi^n, \mathcal{L}(2\phi^{n+1} - \phi^n)) \right) \\ &+ \frac{1}{2} \left((r^{n+1})^2 + (2r^{n+1} - r^n)^2 \right), \end{aligned}$$

and one can obtain $(\phi^{n+1}, \mu^{n+1}, r^{n+1})$ by solving two linear equations with constant coefficients of the form (2.12).

We observe that the modified energy $\tilde{\mathcal{E}}[(\phi^{n+1}, r^{n+1}), (\phi^n, r^n)]$ is an approximation of the original energy $\mathcal{E}[\phi^{n+1}]$ if $(r^{n+1})^2$ is an approximation of $\mathcal{E}_1[\phi^{n+1}]$.

2.2. Gradient Flows of Multiple Functions. We describe below the SAV approach for gradient flows of multiple functions ϕ_1, \dots, ϕ_k ,

$$(2.18) \quad \mathcal{E}[\phi_1, \dots, \phi_k] = \frac{1}{2} \sum_{i,j=1}^k d_{ij}(\phi_i, \mathcal{L}\phi_j) + \mathcal{E}_1[\phi_1, \dots, \phi_k],$$

where \mathcal{L} is a self-adjoint nonnegative linear operator, and the constant matrix $(d_{ij})_{i,j=1,\dots,k}$ is symmetric positive definite. Also, we assume that $\mathcal{E}_1 \geq C_1 > 0$. We consider the gradient flow that contains linear couplings between $\mu_i = \delta\mathcal{E}/\delta\phi_i$. Let \mathcal{G} be a nonpositive dissipation operator and $(g_{ij})_{i,j=1,\dots,k}$ be another symmetric positive definite constant matrix. Denote $U_i = \delta\mathcal{E}_1/\delta\phi_i$, and introduce $r(t) = \sqrt{\mathcal{E}_1}$ as the SAV. The gradient flow is then given by

$$(2.19a) \quad \frac{\partial\phi_i}{\partial t} = \sum_{l=1}^k g_{il}\mathcal{G}\mu_l,$$

$$(2.19b) \quad \mu_i = \sum_{j=1}^k d_{ij}\mathcal{L}\phi_j + \frac{r}{\sqrt{\mathcal{E}_1}}U_i,$$

$$(2.19c) \quad \frac{dr}{dt} = \frac{1}{2\sqrt{\mathcal{E}_1}} \int_{\Omega} U_i \frac{\partial\phi_i}{\partial t} d\mathbf{x}.$$

Taking the inner products of the above three equations with μ_i , $\frac{\partial\phi_i}{\partial t}$, and $2r$, summing over i , and using the facts that \mathcal{L} is self-adjoint and that $d_{ij} = d_{ji}$, we obtain the energy law

$$(2.20) \quad \frac{d}{dt} \mathcal{E}[\phi_1, \dots, \phi_k] = \frac{d}{dt} \left\{ \frac{1}{2} \sum_{i,j=1}^k d_{ij}(\phi_i, \mathcal{L}\phi_j) + \mathcal{E}_1[\phi_1, \dots, \phi_k] \right\} = \sum_{i,l=1}^k g_{il}(\mathcal{G}\mu_i, \mu_l).$$

A simple case with decoupled linear terms, i.e., $d_{ij} = g_{ij} = \delta_{ij}$, is considered in [68]. However, some applications (cf., for example, [30, 8, 9, 16, 11, 57, 24]) involve coupled

linear operators which render the problem very difficult to solve numerically using existing methods. However, we can easily construct simple and accurate schemes using the SAV approach, an example being the following second-order SAV/CN scheme:

(2.21a)

$$\frac{\phi_i^{n+1} - \phi_i^n}{\Delta t} = \sum_{l=1}^k g_{il} \mathcal{G} \mu_l^{n+1/2},$$

(2.21b)
$$\mu_i^{n+1/2} = \frac{1}{2} \sum_{j=1}^k d_{ij} \mathcal{L}(\phi_j^{n+1} + \phi_j^n) + \frac{U_i[\bar{\phi}_1^{n+1/2}, \dots, \bar{\phi}_k^{n+1/2}]}{2\sqrt{\mathcal{E}_1[\bar{\phi}_1^{n+1/2}, \dots, \bar{\phi}_k^{n+1/2}]}}(r^{n+1} + r^n),$$

(2.21c)

$$r^{n+1} - r^n = \int_{\Omega} \sum_{j=1}^k \frac{U_j[\bar{\phi}_1^{n+1/2}, \dots, \bar{\phi}_k^{n+1/2}]}{2\sqrt{\mathcal{E}_1[\bar{\phi}_1^{n+1/2}, \dots, \bar{\phi}_k^{n+1/2}]}}(\phi_j^{n+1} - \phi_j^n) d\mathbf{x},$$

where $\bar{\phi}_j^{n+1/2}$ can be any second-order explicit approximation of $\phi_j(t^{n+1/2})$. We multiply the above three equations with $\Delta t \mu_i^{n+1/2}$, $\phi_i^{n+1} - \phi_i^n$, and $r^{n+1} + r^n$ and take the sum over i . Since \mathcal{L} is self-adjoint and $d_{ij} = d_{ji}$, we have

$$\frac{1}{2} \left(\sum_{j=1}^k d_{ij} \mathcal{L}(\phi_j^{n+1} + \phi_j^n), \phi_i^{n+1} - \phi_i^n \right) = \frac{1}{2} \sum_{j=1}^k d_{ij} [(\mathcal{L}\phi_j^{n+1}, \phi_i^{n+1}) - (\mathcal{L}\phi_j^n, \phi_i^n)],$$

which immediately leads to energy stability. Next, we describe how to implement (2.21) efficiently.

Denoting

$$p_i^n = \frac{U_i[\bar{\phi}_1^{n+1/2}, \dots, \bar{\phi}_k^{n+1/2}]}{\sqrt{\mathcal{E}_1[\bar{\phi}_1^{n+1/2}, \dots, \bar{\phi}_k^{n+1/2}]}}$$

and substituting (2.21b) and (2.21c) into (2.21a), we can eliminate $\mu_i^{n+1/2}$ and r^{n+1} to obtain a coupled linear system of k equations of the form

(2.22)

$$\phi_i^{n+1} - \frac{\Delta t}{2} \sum_{l,j=1}^k g_{il} d_{lj} \mathcal{G} \mathcal{L} \phi_j^{n+1} - \frac{\Delta t}{4} \sum_{j=1}^k (\phi_j^{n+1}, p_j^n) \sum_{l=1}^k g_{il} \mathcal{G} p_l^n = b_i^n, \quad i = 1, \dots, k,$$

where b_i^n includes all known terms in the previous time steps. Let us denote $D = (\frac{\Delta t}{2} d_{ij})_{i,j=1, \dots, k}$, $G = (g_{ij})_{i,j=1, \dots, k}$, and

(2.23)
$$\bar{\phi}^{n+1} = (\phi_1^{n+1}, \dots, \phi_k^{n+1})^T, \quad \bar{b}^n = (b_1^n, \dots, b_k^n)^T,$$

$$\bar{u} = \frac{\Delta t}{4} \left(\sum_{l=1}^k g_{1l} \mathcal{G} p_l^n, \dots, \sum_{l=1}^k g_{kl} \mathcal{G} p_l^n \right), \quad \bar{v} = (p_1^n, \dots, p_k^n).$$

The above system can be written in the matrix form

(2.24)
$$(\mathcal{A} + \bar{u} \bar{v}^T) \bar{\phi}^{n+1} = \bar{b}^n,$$

where the operator \mathcal{A} is defined by

(2.25)
$$\mathcal{A} \bar{\phi}^{n+1} = \bar{\phi}^{n+1} - \mathcal{G} \mathcal{L} \mathcal{G} D \bar{\phi}^{n+1}.$$

The above equation can be solved using the Sherman–Morrison–Woodbury formula [39],

$$(2.26) \quad (A + UV^T)^{-1} = A^{-1} - A^{-1}U(I + V^T A^{-1}U)^{-1}V^T A^{-1},$$

where A is an $n \times n$ matrix, U and V are $n \times k$ matrices, and I is the $k \times k$ identity matrix. We note that if $k \ll n$ and A can be inverted efficiently, the Sherman–Morrison–Woodbury formula provides an efficient algorithm to invert the perturbed matrix $A + UV^T$. The system (2.24) corresponds to a case where U and V are $n \times 1$ vectors, so it can be efficiently solved using (2.26).

It remains to describe how to solve the linear system $\mathcal{A}\bar{\phi} = \bar{b}$ efficiently. Since D and G are both symmetric positive definite, we first compute the eigendecomposition of G as $G = E_1 \Gamma E_1^T$, where E_1 is orthogonal and Γ is diagonal, and obtain $G^{1/2} = E_1 \Gamma^{1/2} E_1^T$. Then, we write $GD = G^{1/2}(G^{1/2}DG^{1/2})G^{-1/2}$ and compute another eigendecomposition of the symmetric positive definite matrix $G^{1/2}DG^{1/2} = E_2 \Lambda E_2^T$, where E_2 is orthogonal and $\Lambda = \text{diag}(\lambda_1, \dots, \lambda_k)$. Let $E = G^{1/2}E_2$. The eigendecomposition of GD is thus written as $GD = E \Lambda E^{-1}$. Setting $\bar{\psi} = E^{-1}\bar{\phi}$, we have

$$\mathcal{A}\bar{\phi} = \bar{\phi} - \mathcal{G} \mathcal{L} E \Lambda E^{-1} \bar{\phi} = E(I - \mathcal{G} \mathcal{L} \Lambda) \bar{\psi}.$$

Hence, $\mathcal{A}\bar{\phi} = \bar{b}$ decouples into a sequence of elliptic equations:

$$(2.27) \quad \psi_i - \lambda_i \mathcal{G} \mathcal{L} \psi_i = (E^{-1} \bar{b})_i, \quad i = 1, \dots, k.$$

To summarize, $\mathcal{A}\bar{\phi} = \bar{b}$ can be efficiently solved as follows:

- Compute the eigendecomposition $G = E_1 \Gamma E_1^T$, followed by $G^{1/2}$. Then compute another eigendecomposition $G^{1/2}DG^{1/2} = E_2 \Lambda E_2^T$.
- Compute $E = G^{1/2}E_2$ and $E^{-1}\bar{b}$.
- Solve the decoupled equations (2.27).
- Finally, the solution is $\bar{\phi} = E\bar{\psi}$.

In summary, we have the following theorem.

THEOREM 2.3. *The scheme (2.21) is second-order accurate and unconditionally energy stable in the sense that*

$$\begin{aligned} & \frac{1}{\Delta t} \left[\frac{1}{2} \sum_{i,j=1}^k d_{ij} (\mathcal{L}\phi_j^{n+1}, \phi_i^{n+1}) + (r^{n+1})^2 \right] - \frac{1}{\Delta t} \left[\frac{1}{2} \sum_{i,j=1}^k d_{ij} (\mathcal{L}\phi_j^n, \phi_i^n) + (r^n)^2 \right] \\ & = \sum_{i=1}^k (\mathcal{G}\mu_i, \mu_i), \end{aligned}$$

and one can obtain r^{n+1} and $(\phi_j^{n+1}, \mu_j^{n+1})_{1 \leq j \leq k}$ by solving two sequences of decoupled linear equations with constant coefficients of the form (2.27).

2.3. Full Discretization. To simplify the presentation, we have only discussed the time discretization above. However, since the stability proofs of SAV schemes are all variational, they can be straightforwardly extended to fully discrete SAV schemes with Galerkin finite element methods or Galerkin spectral methods, or even finite difference methods with summation by parts.

3. Numerical Validation. In this section, we apply the SAV/CN and SAV/BDF schemes to several gradient flows to demonstrate the efficiency and accuracy of the SAV approach. In all examples, we assume periodic boundary conditions and use a Fourier spectral method for space variables.

3.1. Allen–Cahn, Cahn–Hilliard, and Fractional Cahn–Hilliard Equations. The Allen–Cahn [2] and Cahn–Hilliard equations [13, 14] are widely used in the study of interfacial dynamics [2, 62, 4, 42, 46, 52, 53, 76, 1]. They are built with the free energy

$$(3.1) \quad \mathcal{E}[\phi] = \int \frac{1}{2} |\nabla \phi|^2 + \frac{1}{4\epsilon^2} (1 - \phi^2)^2 d\mathbf{x}.$$

We consider the $H^{-\alpha}$ gradient flow, which leads to the fractional Cahn–Hilliard equation

$$(3.2) \quad \frac{\partial \phi}{\partial t} = -\gamma (-\Delta)^\alpha \left(-\Delta \phi - \frac{1}{\epsilon^2} \phi(1 - \phi^2) \right), \quad 0 \leq s \leq 1.$$

Here, the fractional Laplacian operator $(-\Delta)^\alpha$ is defined via Fourier expansion. More precisely, if $\Omega = (0, 2\pi)^2$, then we can express $u \in L^2(\Omega)$ as

$$u = \sum_{m,n} \hat{u}_{mn} e^{imx+iny},$$

so the fractional Laplacian is defined as

$$(-\Delta)^\alpha u = \sum (m^2 + n^2)^\alpha \hat{u}_{mn} e^{imx+iny}.$$

When $\alpha = 0$ (L^2 gradient flow), (3.2) is the standard Allen–Cahn equation; when $\alpha = 1$, it becomes the standard Cahn–Hilliard equation.

To apply our schemes (2.13) or (2.16) to (3.2), we specify the operators \mathcal{L} , \mathcal{G} and the energy \mathcal{E}_1 as

$$(3.3) \quad \mathcal{L} = -\Delta + \frac{\beta}{\epsilon^2}, \quad \mathcal{G} = -(-\Delta)^\alpha, \quad \mathcal{E}_1 = \frac{1}{4\epsilon^2} \int_{\Omega} (\phi^2 - 1 - \beta)^2 d\mathbf{x};$$

then we have

$$U[\phi] = \frac{\delta \mathcal{E}_1}{\delta \phi} = \frac{1}{\epsilon^2} \phi (\phi^2 - 1 - \beta).$$

REMARK 3.1. *In the above, β is a suitable parameter to ensure that there is enough dissipation in the implicit part of the scheme. The effect of using $\beta > 0$ is similar to the stabilization in the usual semi-implicit scheme [69]. For problems with free energy dominated by the nonlinear part such as the case above, a suitable splitting is very important to ensure the accuracy of SAV schemes without using exceedingly small time steps.*

We illustrate this by a typical example. Consider the standard Cahn–Hilliard equation using the SAV/CN scheme in $[0, 2\pi]$. The parameters in the equation are chosen as $\epsilon = 0.1$, $\gamma = 1$. The initial condition is $\phi(x, 0) = 0.2 \sin x$. The space is discretized by a Fourier Galerkin method with $N = 2^{11}$.

Let us compare the results of $\beta = 0$ (without stabilization) and $\beta = 1$ (with stabilization) with two different time steps $\Delta t = 10^{-4}$ and $\Delta t = 4 \times 10^{-3}$. The solution at $T = 0.1$ is plotted in Figure 1. It is clear that with small Δt , the solutions are indistinguishable, regardless of whether we incorporate stabilization. However, with large Δt , the scheme with stabilization leads to the correct solution, but the scheme without stabilization does not.

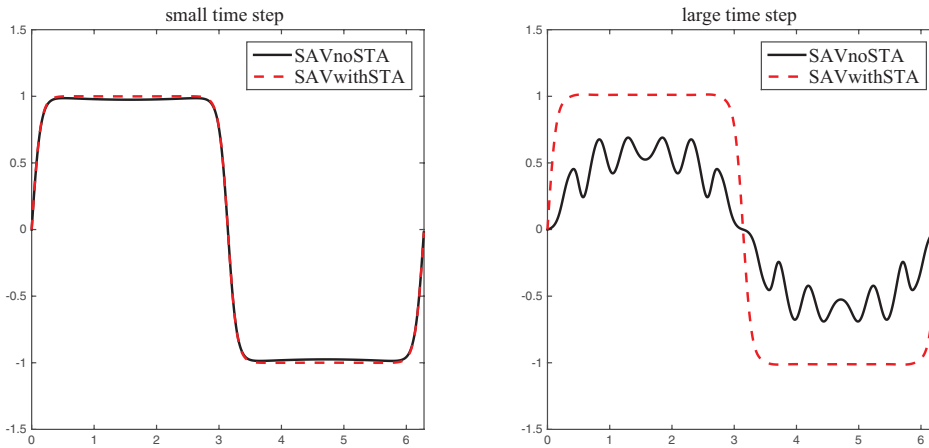


Fig. 1 (Effect of stabilization.) The solution at $T = 0.1$. Left: $\Delta t = 10^{-4}$. Right: $\Delta t = 4 \times 10^{-3}$. The red dashed lines represent solutions with stabilization, while the black solid lines represent solutions without stabilization.

Table 1 (Example 1.) Errors and convergence rates of the SAV/CN and SAV/BDF schemes for the Cahn–Hilliard equation.

Scheme		$\Delta t=1.6e-4$	$\Delta t=8e-5$	$\Delta t=4e-5$	$\Delta t=2e-5$	$\Delta t=1e-5$
SAV/CN	Error	1.74e-7	4.54e-8	1.17e-8	2.94e-9	2.01e-10
	Rate	-	1.93	1.96	1.99	2.01
SAV/BDF	Error	1.38e-6	3.72e-7	9.63e-8	2.43e-8	5.98e-9
	Rate	-	1.89	1.95	1.99	2.02

Example 1. (Convergence rate of the SAV/CN scheme for the standard Cahn–Hilliard equation.) We choose the computational domain as $[0, 2\pi]^2$, $\epsilon = 0.1$, and $\gamma = 1$. The initial data is chosen to be smooth: $\phi(x, y, 0) = 0.05 \sin(x) \sin(y)$.

We use the Fourier Galerkin method for spatial discretization with $N = 2^7$, and choose $\beta = 1$. To compute a reference solution, we use the fourth-order exponential time differencing Runge–Kutta method (ETDRK4)* [21] with Δt sufficiently small. The numerical errors at $t = 0.032$ for SAV/CN and SAV/BDF are shown in Table 1, where we can observe the second-order convergence for both schemes.

Example 2. We solve a benchmark problem for the Allen–Cahn equation (see [17]). Consider a two-dimensional domain $(-128, 128)^2$ with a circle of radius $R_0 = 100$. In other words, the initial condition is given by

$$(3.4) \quad \phi(x, y, 0) = \begin{cases} 1, & x^2 + y^2 < 100^2, \\ 0, & x^2 + y^2 \geq 100^2. \end{cases}$$

By mapping the domain to $(-1, 1)^2$, the parameters in the Allen–Cahn equation are given by $\gamma = 6.10351 \times 10^{-5}$ and $\epsilon = 0.0078$.

*Although ETDRK4 has higher order of accuracy, it does not guarantee energy stability, and the implementation can be difficult since it requires us to calculate the matrix exponential.

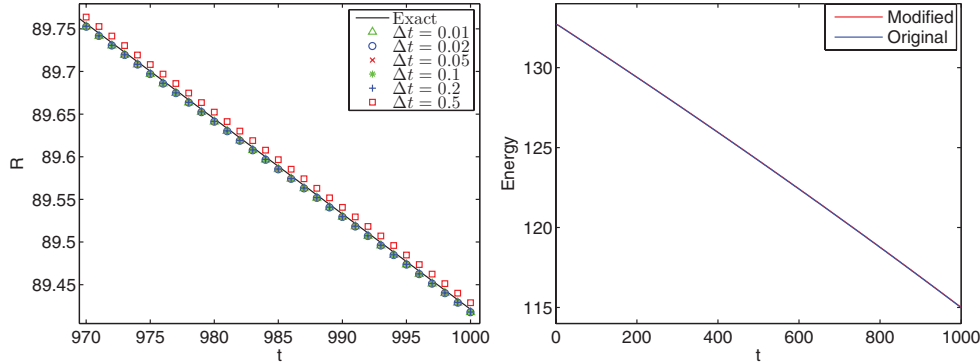


Fig. 2 (Example 2.) The evolution of radius $R(t)$ and the free energy (both original and modified). For the free energy, $\Delta t = 0.5$.

In the sharp interface limit ($\epsilon \rightarrow 0$, which is suitable because the chosen ϵ is small), the radius at time t is given by

$$(3.5) \quad R = \sqrt{R_0^2 - 2t}.$$

We use the Fourier Galerkin method to express ϕ as

$$(3.6) \quad \phi = \sum_{n_1, n_2 \leq N} \hat{\phi}_{n_1 n_2} e^{i\pi(n_1 x + n_2 y)},$$

with $N = 2^9$. We choose $\beta = 1$ and let the time step Δt vary. The computed radius $R(t)$ using the SAV/CN scheme is plotted in Figure 2. We observe that $R(t)$ keeps monotonically decreasing and is very close to the sharp interface limit value, even when we choose a relatively large Δt . In [69] this benchmark problem is solved using different stabilization methods. Our result proves to be much better than the result in that work, where the oscillation around the limit value is apparent, even though the time step is reduced to $\Delta t = 10^{-3}$. We also plot the original energy and the modified energy $\frac{1}{2}(\phi^n, \mathcal{L}\phi^n) + (r^n)^2$ in Figure 2 for $\Delta t = 0.5$, and find that they are very close.

Example 3. (Comparison of the SAV/CN and IEQ/CN schemes for the Allen–Cahn equation in one dimension.) The parameters are the same as in the first example. The domain is chosen as $[0, 2\pi]$, discretized by the finite difference method with $N = 2^{10}$. The initial condition $\phi(x, 0)$ is now a randomly generated function. The reference solution is also obtained using ETDRK4.

We plot the numerical results at $T = 0.1$ and $T = 1$ using the SAV/CN and IEQ/CN schemes in Figure 3. We used two different time steps $\Delta t = 10^{-4}$, 10^{-3} . We observe that with $\Delta t = 10^{-4}$, both the SAV/CN scheme and the IEQ/CN scheme agree well with the reference solution. However, with $\Delta t = 10^{-3}$, the solution using the SAV/CN scheme still agrees well with the reference solution at both $T = 0.1$ and $T = 1$, while the solution obtained by the IEQ/CN scheme has visible differences with the reference solution and violates the maximum principle $|\phi| \leq 1$. This example clearly indicates that the SAV/CN scheme is more accurate than the IEQ/CN scheme, in addition to its easy implementation.

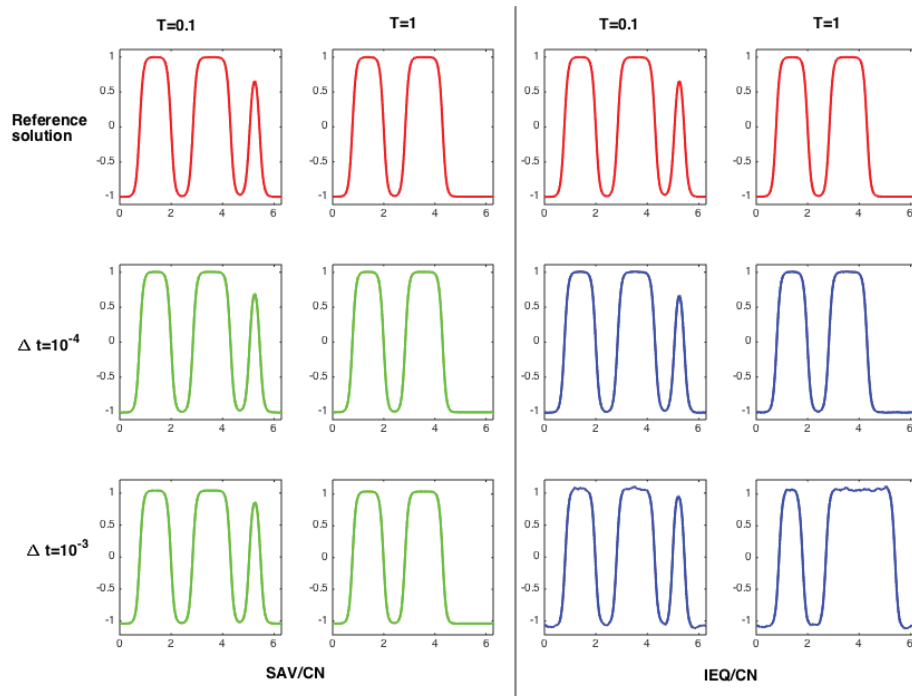


Fig. 3 (Example 3.) Comparison of the SAV/CN and IEQ/CN schemes.

Example 4. We examine the effect of the fractional dissipation mechanism on the phase separation and coarsening process. Consider the fractional Cahn–Hilliard equation in $[0, 2\pi]^2$. We fix $\epsilon = 0.04$ and take the fractional power α to be 0.1, 0.5, 1, respectively. We use the Fourier Galerkin method with $N = 2^7$, and the time step $\Delta t = 8 \times 10^{-6}$. The initial value is the sum of a randomly generated function $\phi_0(x, y)$ with the average of ϕ ,

$$\bar{\phi} = \frac{1}{4\pi^2} \int_{0 \leq x, y \leq 2\pi} \phi \, dx dy,$$

chosen as 0.25, 0, and -0.25 , respectively.

We used the SAV/BDF scheme to compute the configuration at $T = 0.032$, which is shown in Figure 4. We observe that regardless of $\bar{\phi}$, when α is smaller, the phase separation and coarsening process is slower, which is consistent with the results in [1].

3.2. Phase Field Crystals. We now consider gradient flows of $\phi(\mathbf{x})$ that describe modulated structures. Free energy of this kind was first found in Brazovskii’s work [12], known as the Landau–Brazovskii model. Since then, the free energy, including many variants, has been adopted to study various physical systems (see, for example, [37, 3, 40, 73]). A usual free energy takes the form

$$(3.7) \quad \mathcal{E}(\phi) = \int_{\Omega} \left\{ \frac{1}{4} \phi^4 + \frac{1-\epsilon}{2} \phi^2 - |\nabla \phi|^2 + \frac{1}{2} (\Delta \phi)^2 \right\} d\mathbf{x},$$

subject to a constraint that the average $\bar{\phi}$ remains constant. This constraint can be automatically satisfied with an H^{-1} gradient flow, which is also referred to as a phase field crystals model because it is widely adopted in the dynamics of crystallization

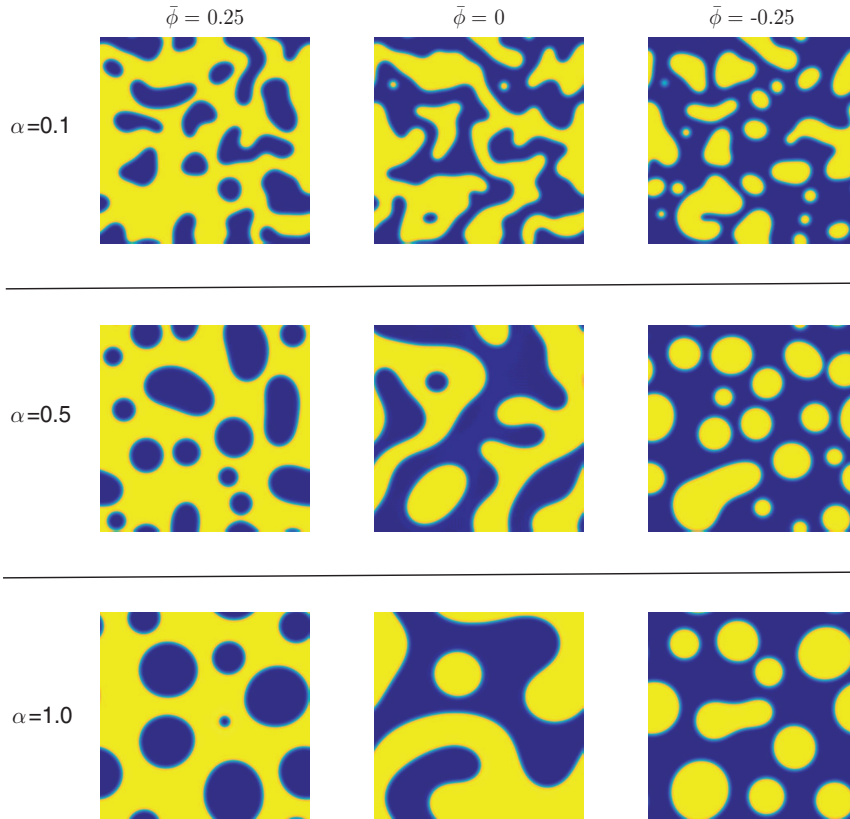


Fig. 4 (Example 4.) Configurations at time $T = 0.032$ with random initial condition for different values of fractional order α and mean $\bar{\phi}$.

[27, 26, 28]. To demonstrate the flexibility of the SAV approach, we will focus on a free energy with a nonlocal kernel. Specifically, we replace the Laplacian by a nonlocal linear operator \mathcal{L}_δ [71],

$$\mathcal{L}_\delta \phi(\mathbf{x}) = \int_{\mathcal{B}(\mathbf{x}, \delta)} \rho_\delta(|\mathbf{y} - \mathbf{x}|) (\phi(\mathbf{y}) - \phi(\mathbf{x})) d\mathbf{y},$$

leading to the free energy

$$(3.8) \quad \mathcal{E}(\phi) = \int_{\Omega} \left\{ \frac{1}{4} \phi^4 + \frac{1-\epsilon}{2} \phi^2 + \phi \mathcal{L}_\delta \phi + \frac{1}{2} (\mathcal{L}_\delta \phi)^2 \right\} d\mathbf{x}.$$

Let the dissipation mechanism be given by $\mathcal{G} = \mathcal{L}_\delta$. Then we obtain the following gradient flow:

$$(3.9) \quad \frac{\partial \phi}{\partial t} = \mathcal{L}_\delta (\mathcal{L}_\delta^2 \phi + 2\mathcal{L}_\delta \phi + (1-\epsilon)\phi + \phi^3).$$

For the above problem, it is difficult to solve the linear system resulting from the IEQ approach, but it can be easily implemented with the SAV approach.

Let Ω be a rectangular domain $[0, 2\pi)^2$ with periodic boundary conditions; the eigenvalues of \mathcal{L} can be expressed explicitly. In fact, it is easy to check that for any integers m and n , $e^{imx+iny}$ is an eigenfunction of \mathcal{L}_δ and the corresponding eigenvalue is given by

$$\lambda_\delta(m, n) = \int_0^\delta r \rho_\delta(r) \int_0^{2\pi} (\cos(r(m \cos \theta + n \cos \theta)) - 1) d\theta dr,$$

which can be evaluated efficiently using a hybrid algorithm [25]. We choose

$$\rho_\delta(|\mathbf{x} - \mathbf{x}'|) = c_1 \frac{2(4 - \alpha_1)}{\pi} \frac{1}{\delta^{4-\alpha_1} r^{\alpha_1}} - c_2 \frac{2(4 - \alpha_2)}{\pi} \frac{1}{\delta^{4-\alpha_2} r^{\alpha_2}},$$

with $c_1 = 20$, $c_2 = 19$, $\alpha_1 = 3$, $\alpha_2 = 0$, and $\delta = 2$. Numerical results indicate that all eigenvalues are negative, which ensures the nonlocal operator \mathcal{L}_δ is negative-semidefinite.

We have applied the SAV/CN and SAV/BDF schemes to (3.9). As a comparison, we also implemented the following stabilized semi-implicit (SSI) scheme used in [19]:

$$\begin{aligned} \frac{\phi^{n+1} - \phi^n}{\Delta t} &= (1 - \epsilon) \mathcal{L}_\delta \phi^{n+1} + 2\mathcal{L}_\delta^2 \phi^{n+1} + \mathcal{L}_\delta^3 \phi^{n+1} + (\phi^n)^3 \\ &\quad + a_1(1 - \epsilon) \mathcal{L}_\delta(\phi^{n+1} - \phi^n) - 2a_2 \mathcal{L}_\delta^2(\phi^{n+1} - \phi^n) + a_3 \mathcal{L}_\delta^3(\phi^{n+1} - \phi^n). \end{aligned}$$

Specifically, we choose $a_1 = 0$, $a_2 = 1$, and $a_3 = 0$ which satisfy the parameter constraints provided in [19].

For the SAV schemes, we specify the linear nonnegative operator as $\mathcal{L} = \mathcal{L}_\delta^2 + 2\mathcal{L}_\delta + I$. The time step is fixed at $\Delta t = 1$.

Example 5. We consider (3.9) in the two-dimensional domain $[0, 50] \times [0, 50]$ with periodic boundary conditions. Fix $\epsilon = 0.025$ and $\phi = 0.07$. The Fourier Galerkin method is used for spatial discretization with $N = 2^7$.

The residual of (3.9) is defined so that it measures how far the solution is away from the steady state,

$$\text{residual} = \|\mathcal{L}_\delta(\mathcal{L}_\delta^2 \phi + 2\mathcal{L}_\delta \phi + (1 - \epsilon)\phi + \phi^3)\|_2^2.$$

The initial value possesses a square structure, drawn in the first row in Figure 5, and the configurations at $T = 2400$ and 4800 are shown in the other two rows. There is no visible difference among the results for all three schemes at $T = 2400$. However, for both SAV schemes, the system eventually evolves to a stable hexagonal structure, while for the SSI scheme it remains as the unstable square structure. We also plot the free energy and residual as functions of time for the three schemes (see Figure 6). For the SSI scheme, the residue starts to increase when $T > 3000$, and the free energy eventually increases, violating the energy law. On the other hand, the free energy curves for both SAV schemes remain dissipative, with no visible difference between them. This example clearly shows that our SAV schemes have much better stability and accuracy than the SSI scheme for the nonlocal model (3.9).

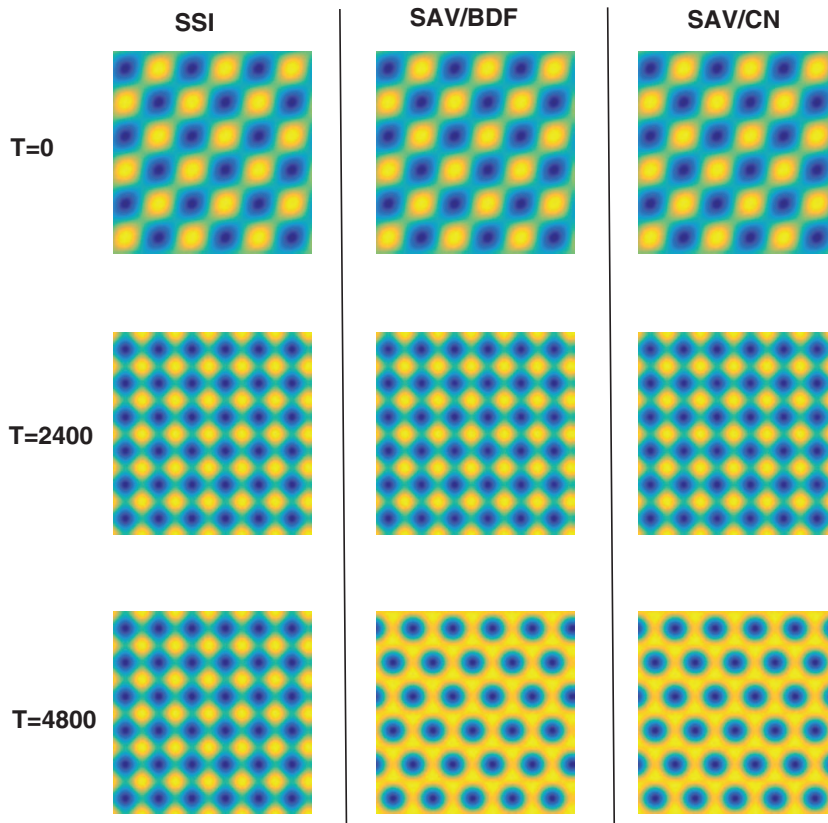


Fig. 5 (Example 5.) Configuration evolutions for nonlocal phase field crystals (NPFC) model by three schemes.

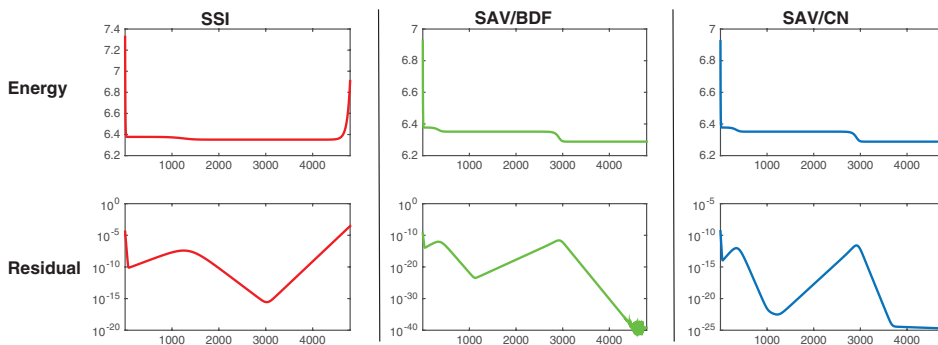


Fig. 6 (Example 5.) Energy evolutions and residual evolutions for NPFC models using three schemes.

4. Higher-Order SAV Schemes and Adaptive Time Stepping. We describe below how to construct higher-order schemes for gradient flows by combining the SAV approach with higher-order BDF schemes, and also how to implement adaptive time stepping to further increase the computational efficiency.

4.1. Higher-Order SAV Schemes. For the reformulated system (2.1c)–(2.1b), we can easily use the SAV approach to construct BDF- k ($k \geq 3$) schemes. Since BDF- k ($k \geq 3$) schemes are not A-stable for ODEs, they will not be unconditionally stable. We will focus on BDF3 and BDF4 schemes below, since for $k > 4$, the resulting BDF- k schemes do not appear to be stable.

The SAV/BDF3 scheme is given by

$$\begin{aligned} \frac{11\phi^{n+1} - 18\phi^n + 9\phi^{n-1} - 2\phi^{n-2}}{6\Delta t} &= \mathcal{G}\mu^{n+1}, \\ \mu^{n+1} &= \mathcal{L}\phi^{n+1} + \frac{r^{n+1}}{\sqrt{\mathcal{E}_1[\bar{\phi}^{n+1}]}} U[\bar{\phi}^{n+1}], \\ 11r^{n+1} - 18r^n + 9r^{n-1} - 2r^{n-2} \\ &= \int_{\Omega} \frac{U[\bar{\phi}^{n+1}]}{2\sqrt{\mathcal{E}_1[\bar{\phi}^{n+1}]}} (11\phi^{n+1} - 18\phi^n + 9\phi^{n-1} - 2\phi^{n-2}) d\mathbf{x}, \end{aligned}$$

where $\bar{\phi}^{n+1}$ is a third-order explicit approximation to $\phi(t_{n+1})$. The SAV/BDF4 scheme is given by

$$\begin{aligned} \frac{25\phi^{n+1} - 48\phi^n + 36\phi^{n-1} - 16\phi^{n-2} + 3\phi^{n-3}}{12\Delta t} &= \mathcal{G}\mu^{n+1}, \\ \mu^{n+1} &= \mathcal{L}\phi^{n+1} + \frac{r^{n+1}}{\sqrt{\mathcal{E}_1[\bar{\phi}^{n+1}]}} U[\bar{\phi}^{n+1}], \\ 25r^{n+1} - 48r^n + 36r^{n-1} - 16r^{n-2} + 3r^{n-3} \\ &= \int_{\Omega} \frac{U[\bar{\phi}^{n+1}]}{2\sqrt{\mathcal{E}_1[\bar{\phi}^{n+1}]}} (25\phi^{n+1} - 48\phi^n + 36\phi^{n-1} - 16\phi^{n-2} + 3\phi^{n-3}) d\mathbf{x}, \end{aligned}$$

where $\bar{\phi}^{n+1}$ is a fourth-order explicit approximation to $\phi(t_{n+1})$.

To obtain $\bar{\phi}^{n+1}$ in BDF3, we can use the extrapolation (BDF3A),

$$\bar{\phi}^{n+1} = 3\phi^n - 3\phi^{n-1} + \phi^{n-2},$$

or prediction by one BDF2 step (BDF3B),

$$\bar{\phi}^{n+1} = \text{BDF2}\{\phi^n, \phi^{n-1}, \Delta t\}.$$

Similarly, to obtain $\bar{\phi}^{n+1}$ in BDF4, we can do the extrapolation (BDF4A)

$$\bar{\phi}^{n+1} = 4\phi^n - 6\phi^{n-1} + 4\phi^{n-2} - \phi^{n-3},$$

or prediction with one step of BDF3A (BDF4B),

$$\bar{\phi}^{n+1} = \text{BDF3}\{\phi^n, \phi^{n-1}, \phi^{n-2}, \Delta t\}.$$

It can be seen that using the prediction with a lower-order BDF step will double the total computation cost.

Example 6. We take the Cahn–Hilliard equation as an example to demonstrate the numerical performance of the SAV/BDF3 and SAV/BDF4 schemes. We fix the computational domain as $[0, 2\pi]^2$ and $\epsilon = 0.1$. We use the Fourier Galerkin method for spatial discretization with $N = 2^7$. The initial data is $u_0(x, y) = 0.05 \sin(x) \sin(y)$.

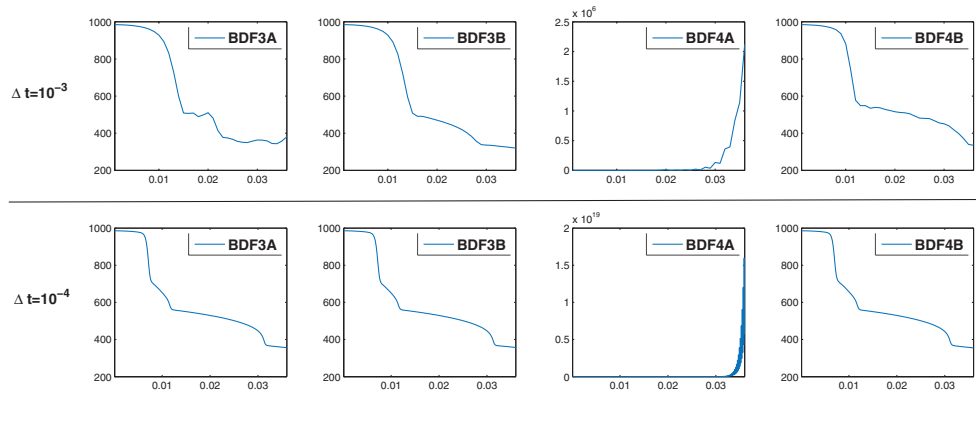


Fig. 7 (Example 6.) Energy evolution for BDF3 and BDF4 schemes.

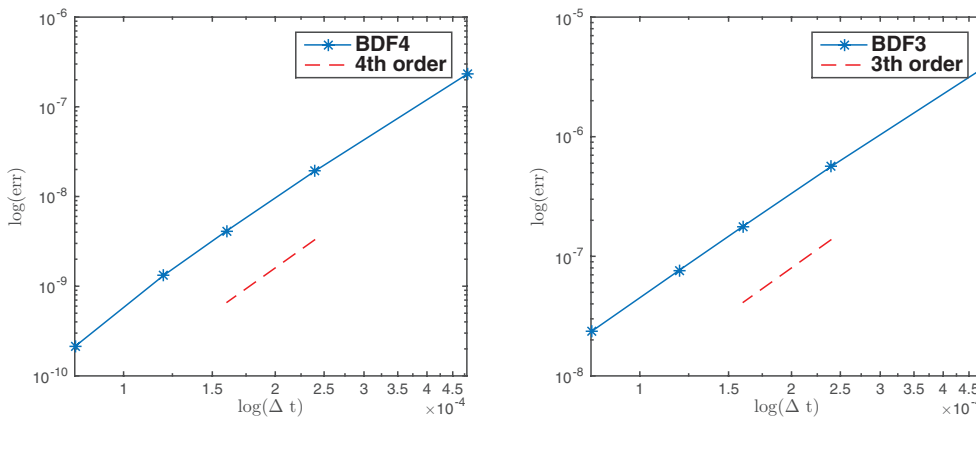


Fig. 8 (Example 6.) Numerical convergence of BDF3 and BDF4.

We first examine the energy evolution of BDF3A, BDF3B, BDF4A, and BDF4B with $\Delta t = 10^{-3}$ and $\Delta t = 10^{-4}$, respectively. The numerical results are shown in Figure 7. We find that BDF4A is unstable and BDF3A shows oscillations in energy with $\Delta t = 10^{-3}$. Hence, in what follows, we will focus on BDF3B and BDF4B, which are abbreviated by BDF3 and BDF4.

Next, we examine the numerical errors of BDF3 and BDF4, plotted in Figure 8. The reference solution is obtained by ETDRK4 with a sufficiently small time step. It can be observed that BDF3 and BDF4 schemes achieve third-order and fourth-order convergence rates, respectively.

We then compare the numerical results of BDF2, BDF3, and BDF4.

The energy evolution and the configuration at $t = 0.016$ are shown in Figure 9 (for the first row $\Delta t = 10^{-3}$, and for the second row $\Delta t = 10^{-4}$). We observe that at $\Delta t = 10^{-4}$, all schemes lead to the correct solution although there is some visible difference in the energy evolution between BDF2 and the other higher-order schemes, but at $\Delta t = 10^{-3}$, only BDF4 leads to the correct solution. The above results indicate that higher-order SAV schemes can be used to improve accuracy.

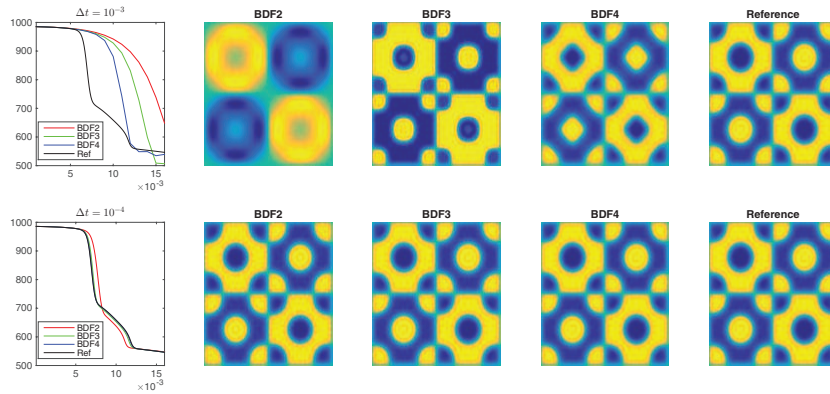


Fig. 9 (Example 6.) Comparison of BDF2, BDF3, and BDF4. Upper: $\Delta t = 10^{-3}$. Lower: $\Delta t = 10^{-4}$. The line graphs give the energy evolution. All the snapshots are taken at $t = 0.016$.

4.2. Adaptive Time Stepping. In many situations, the energy and solution of gradient flows can vary drastically in a certain time interval, but only slightly elsewhere. One main advantage of unconditional energy stable schemes is that they can be easily implemented with an adaptive time stepping strategy so that the time step is dictated only by accuracy rather than by stability as with conditionally stable schemes.

There are several adaptive strategies for the gradient flows. Here, we follow the adaptive time stepping strategy in [64] summarized in Algorithm 1, which has been shown to be effective for Allen–Cahn equations. In Step 4 and Step 6 of Algorithm 1, the formula for updating the time step size is given by

$$(4.1) \quad A_{\Phi}(e, \tau) = \rho \left(\frac{\text{tol}}{e} \right)^{1/2} \tau,$$

along with restriction of the minimum and maximum time steps. In the above, ρ is a default safety coefficient, tol is a reference tolerance, and e is the relative error at each time level computed in Step 3 in Algorithm 1. In the following example, we choose $\rho = 0.9$ and $\text{tol} = 10^{-3}$. The minimum and maximum time steps are taken as $\tau_{\min} = 10^{-5}$ and $\tau_{\max} = 10^{-2}$, respectively. The initial time step is taken as τ_{\min} .

Algorithm 1 Time step adaptive procedure.

Given: U^n, τ_n .

Step 1. Compute U_1^{n+1} by the first-order SAV scheme with τ_n .

Step 2. Compute U_2^{n+1} by the second-order SAV scheme with τ_n .

Step 3. Calculate $e_{n+1} = \frac{\|U_1^{n+1} - U_2^{n+1}\|}{\|U_2^{n+1}\|}$.

Step 4. if $e_{n+1} > \text{tol}$, **then**

Recalculate time step $\tau_n \leftarrow \max\{\tau_{\min}, \min\{A_{\Phi}(e_{n+1}, \tau_n), \tau_{\max}\}\}$.

Step 5. goto Step 1

Step 6. else

Update time step $\tau_{n+1} \leftarrow \max\{\tau_{\min}, \min\{A_{\Phi}(e_{n+1}, \tau_n), \tau_{\max}\}\}$.

Step 7. endif

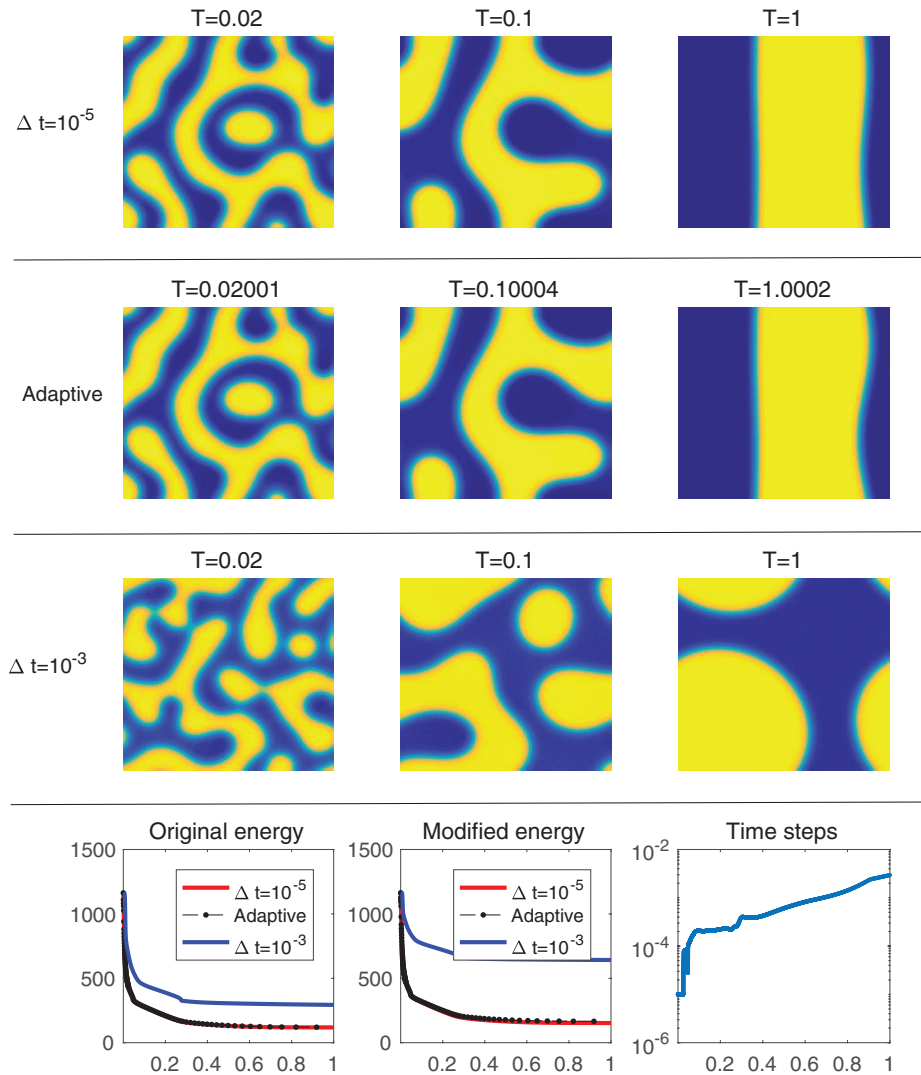


Fig. 10 (Example 7.) Numerical comparisons among small time steps, adaptive time steps, and large time steps.

We use the two-dimensional Cahn–Hilliard equation as an example to demonstrate the performance of the time adaptivity.

Example 7. Consider the two-dimensional Cahn–Hilliard equation on $[0, 2\pi] \times [0, 2\pi]$ with periodic boundary conditions and random initial data. We take $\epsilon = 0.1$ and use the Fourier-spectral method with $N_x = N_y = 256$.

As comparison, we compute a reference solution using the SAV/CN scheme with a small uniform time step $\tau = 10^{-5}$ and a large uniform time step $\tau = 10^{-3}$. Snapshots of phase evolutions, original energy evolutions, and modified energy evolution, and the size of time steps in the adaptive experiment, are shown in Figure 10. It can be observed that the adaptive time solutions given in the middle row are in good

agreement with the reference solution presented in the top row. However, the solutions with large time step are far away from the reference solution. This is also indicated by both the original energy evolutions and the modified energy evolutions. Note also that the time step changes accordingly with the energy evolution. There are almost three orders of magnitude variation in the time step, which indicates that the adaptive time stepping for the SAV schemes is very effective.

5. Various Applications of the SAV Approach. We emphasize that the SAV approach can be applied to a large class of gradient flows. In this section, we shall apply the SAV approach to several challenging gradient flows with different characteristics and show that the SAV approach leads to very efficient and accurate energy stable numerical schemes for these problems and for those with similar characteristics.

5.1. Gradient Flows with Nonlocal Free Energy. In most gradient flows, the governing free energy is local, i.e., can be written as an integral of functions about order parameters and their derivatives on a domain Ω . In fact, many of these models can be derived as approximations of density functional theory (DFT) (see, for example, [54]) that take a nonlocal form. Recently, there has been growing interest in using nonlocal models to describe phenomena that are difficult to capture in local models. Examples include peridynamics [71] and quasi-crystals [5, 7, 43].

Although more complicated forms are possible, we consider the following free energy functional that covers those in the models mentioned above,

$$\begin{aligned} \mathcal{E}[\phi] &= \int_{\Omega} \left(F(\phi) + \frac{1}{2} \phi \mathcal{L} \phi \right) d\mathbf{x} + \frac{1}{2} \int_{\Omega} \int_{\Omega} K(|\mathbf{x} - \mathbf{x}'|) \phi(\mathbf{x}) \phi(\mathbf{x}') d\mathbf{x}' d\mathbf{x} \\ (5.1) \quad &:= (F(\phi), 1) + \frac{1}{2} (\mathcal{L} \phi, \phi) + \frac{1}{2} (\phi, \mathcal{L}_n \phi), \end{aligned}$$

where \mathcal{L} is a local symmetric positive differential operator, $K(|\mathbf{x} - \mathbf{x}'|)$ is a kernel function, $F(\phi)$ is a nonlinear (local) free energy density, and the operator \mathcal{L}_n is given by

$$(5.2) \quad (\mathcal{L}_n \phi)(\mathbf{x}) = \int K(|\mathbf{x} - \mathbf{x}'|) \phi(\mathbf{x}') d\mathbf{x}'.$$

Then, the corresponding gradient flow associated with energy dissipation \mathcal{G} is

$$(5.3) \quad \frac{\partial \phi}{\partial t} = \mathcal{G} (\mathcal{L} \phi + \mathcal{L}_n \phi + f(\phi)),$$

where $f(\phi) = F'(\phi)$.

In general, \mathcal{L} may not be positive and can be controlled by the nonlinear term $F(\phi)$, as in the nonlocal models we mentioned above. In this case, we may place part of the nonlocal term together with the nonlinear term, and then handle the nonlocal term explicitly in the SAV approach. More precisely, we split $\mathcal{L}_n = \mathcal{L}_{n1} + \mathcal{L}_{n2}$ and set

$$\mathcal{E}_1(\phi) = \frac{1}{2} (\mathcal{L} \phi, \phi) + \frac{1}{2} (\phi, \mathcal{L}_{n1} \phi), \quad \mathcal{E}_n(\phi) = \frac{1}{2} (\phi, \mathcal{L}_{n2} \phi) + (F(\phi), 1),$$

where we assume that \mathcal{L}_{n1} is positive and $\mathcal{E}_n(\phi) \geq C_0 > 0$. We introduce an SAV

$$r(t) = \sqrt{\mathcal{E}_n(\phi)},$$

and rewrite the gradient flow (5.3) as

$$(5.4a) \quad \frac{\partial \phi}{\partial t} = \mathcal{G} \left((\mathcal{L} + \mathcal{L}_{n1}) \phi + \frac{r}{\sqrt{\mathcal{E}_n(\phi)}} (\mathcal{L}_{n2} \phi + f(\phi)) \right),$$

$$(5.4b) \quad \frac{dr}{dt} = \frac{1}{2\sqrt{\mathcal{E}_n(\phi)}} \left(\frac{\partial \phi}{\partial t}, \mathcal{L}_{n2}\phi + f(\phi) \right).$$

Then the second-order BDF scheme based on the SAV approach is

$$(5.5a) \quad \frac{3\phi^{n+1} - 4\phi^n + \phi^{n-1}}{2\Delta t} = \mathcal{G}\mu^{n+1},$$

$$(5.5b) \quad \mu^{n+1} = (\mathcal{L} + \mathcal{L}_{n1})\phi^{n+1} + \frac{r^{n+1}}{\sqrt{\mathcal{E}_n[\bar{\phi}^{n+1}]}} (\mathcal{L}_{n2}\bar{\phi}^{n+1} + f(\bar{\phi}^{n+1})),$$

$$(5.5c) \quad 3r^{n+1} - 4r^n + r^{n-1} = \frac{1}{2\sqrt{\mathcal{E}_n[\bar{\phi}^{n+1}]}} (\mathcal{L}_{n2}\bar{\phi}^{n+1} + f(\bar{\phi}^{n+1}), 3\phi^{n+1} - 4\phi^n + \phi^{n-1}).$$

Similarly, it is easy to show that the above scheme is unconditionally energy stable and that the scheme only requires, at each time step, solving two linear systems of the form

$$(5.6) \quad (I - \lambda\Delta t\mathcal{G}(\mathcal{L} + \mathcal{L}_{n1}))\phi = f.$$

In particular, if $\mathcal{L} > \mathcal{L}_n$, a good choice can be $\mathcal{L}_{n1} = 0$ and $\mathcal{L}_{n2} = \mathcal{L}_n$, and we only need to solve equations with common differential operators. Note also that the phase field crystal model considered in section 3.2 is a special case with $\mathcal{L} = 0$ and $\mathcal{L}_{n2} = 0$.

Note that the above problem cannot be easily treated with convex splitting or IEQ approaches.

5.2. Molecular Beam Epitaxial (MBE) without Slope Selection. The energy functional for molecular beam epitaxial (MBE) without slope selection is given by [50]

$$(5.7) \quad \mathcal{E}[\phi] = \int_{\Omega} \left[-\frac{1}{2} \ln(1 + |\nabla\phi|^2) + \frac{\eta^2}{2} |\Delta\phi|^2 \right] d\mathbf{x}.$$

In [18], a first-order linear scheme is proposed, where a stabilized term is added to maintain the energy decaying property. A main difficulty is that the first part of the energy density, $-\frac{1}{2} \ln(1 + |\nabla\phi|^2)$, is unbounded from below, so the IEQ approach cannot be applied. However, the SAV approach is still applicable, and it is analyzed and implemented in [20]. Below we summarize the main points of that work to show how the SAV approach works.

One can show (see [20, Lemma 3.1]) for any $\alpha_0 > 0$, there exists $C_0 > 0$ such that

$$(5.8) \quad \mathcal{E}_1[\phi] = \int_{\Omega} \left[-\frac{1}{2} \ln(1 + |\nabla\phi|^2) + \frac{\alpha}{2} |\Delta\phi|^2 \right] d\mathbf{x} \geq -C_0 \quad \forall \alpha \geq \alpha_0 > 0.$$

Hence, we can choose $\alpha_0 < \alpha < \eta^2$ and split $\mathcal{E}[\phi]$ as

$$\mathcal{E}[\phi] = \mathcal{E}_1[\phi] + \int_{\Omega} \frac{\eta^2 - \alpha}{2} |\Delta\phi|^2 d\mathbf{x}.$$

Now we introduce an SAV

$$r(t) = \sqrt{\int_{\Omega} \frac{\alpha}{2} |\Delta\phi|^2 - \frac{1}{2} \ln(1 + |\nabla\phi|^2) d\mathbf{x} + C_0}$$

and rewrite the gradient flow for MBE as

$$(5.9a) \quad \frac{\partial \phi}{\partial t} + (\eta^2 - \alpha)\Delta^2 \phi + G(\phi)r(t) = 0,$$

$$(5.9b) \quad \frac{dr}{dt} = \frac{1}{2} \int_{\Omega} G(\phi) \frac{\partial \phi}{\partial t} d\mathbf{x},$$

where $G(\phi)$ is given following (2.1c),

$$G(\phi) = \frac{\frac{\delta \mathcal{E}_1[\phi]}{\delta \phi}}{\sqrt{\mathcal{E}_1[\phi]}} = \frac{\alpha \Delta^2 \phi + \nabla \cdot \left(\frac{\nabla \phi}{1 + |\nabla \phi|^2} \right)}{\sqrt{\int_{\Omega} \frac{\alpha}{2} |\Delta \phi|^2 - \frac{1}{2} \ln(1 + |\nabla \phi|^2) d\mathbf{x} + C_0}}.$$

Therefore, we can use the SAV approach to construct, for (5.9), second-order linear, unconditionally energy stable schemes which only require, at each time step, solving two linear equations of the form

$$(I + \Delta t \Delta^2)\phi = f.$$

It is clear that the SAV approach is more efficient and easier to implement than existing energy stable schemes that involve solving nonlinear equations (cf., for instance, [50, 65, 61]). We refer the reader to [20] for more detail on SAV schemes and their numerical validation.

5.3. Q-Tensor Model for Rod-Like Liquid Crystals. In many liquid crystal models, a symmetric traceless second-order tensor $Q \in \mathbb{R}^{3 \times 3}$ is used to describe the orientational order. We consider the Landau-de Gennes free energy [22] that has been applied to study various phenomena, both analytically (see, for example, [55, 59]) and numerically (see, for example, [70, 63, 78]). It can be written as $\mathcal{E}[Q(\mathbf{x})] = \mathcal{E}_b + \mathcal{E}_e$, where

$$(5.10) \quad \mathcal{E}_b = \int_{\Omega} f_b(Q) d\mathbf{x} = \int_{\Omega} \left[\frac{a}{2} \text{tr} Q^2 - \frac{b}{3} \text{tr} Q^3 + \frac{c}{4} (\text{tr} Q^2)^2 \right] d\mathbf{x},$$

$$(5.11) \quad \mathcal{E}_e = \int_{\Omega} \left[\frac{L_1}{2} |\nabla Q|^2 + \frac{L_2}{2} \sum_{k=1}^3 \partial_i Q_{ik} \partial_j Q_{jk} + \frac{L_3}{2} \sum_{k=1}^3 \partial_i Q_{jk} \partial_j Q_{ik} \right] d\mathbf{x}.$$

Ensuring the lower-boundedness requires $c > 0$, $L_1, L_1 + L_2 + L_3 > 0$, so that we have $\mathcal{E}_b, \mathcal{E}_e \geq 0$.

We consider the L^2 gradient flow

$$(5.12) \quad \frac{\partial Q_{ij}}{\partial t} = - \left(\frac{\delta \mathcal{E}}{\delta Q} [Q] \right)_{ij}, \quad 1 \leq i, j \leq 3,$$

with

$$(5.13)$$

$$\left(\frac{\delta \mathcal{E}_b}{\delta Q} [Q] \right)_{ij} = a Q_{ij} - b \left(Q_{ik} Q_{kj} - \frac{1}{3} \text{tr} Q^2 \cdot \delta_{ij} \right) + c \text{tr} Q^2 \cdot Q_{ij},$$

$$(5.14)$$

$$\left(\frac{\delta \mathcal{E}_e}{\delta Q} [Q] \right)_{ij} = -L_1 \Delta Q_{ij} - \frac{L_2 + L_3}{2} \left(\sum_{k=1}^3 (\partial_{ik} Q_{jk} + \partial_{jk} Q_{ik}) - \frac{2}{3} \sum_{k,l=1}^3 \partial_{kl} Q_{kl} \delta_{ij} \right).$$

We can see that the components of Q are coupled both in \mathcal{E}_b and \mathcal{E}_e , which makes it difficult to deal with numerically.

Since we have a positive quartic term $c(\text{tr}Q^2)^2$, we can choose $a_1, C_0 \geq 0$ such that $f_b(Q) - a_1 \text{tr}Q^2/2 + C_0 > 0$. We introduce an SAV

$$r(t) = \sqrt{\mathcal{E}_1} := \sqrt{\mathcal{E}_b(Q) - \int_{\Omega} \frac{a_1}{2} \text{tr}Q^2 d\mathbf{x} + C_0}.$$

Let \mathcal{L} be defined as

$$\mathcal{L}Q = a_1Q + \frac{\delta\mathcal{E}_e}{\delta Q}[Q],$$

where $(\delta\mathcal{E}_e/\delta Q)[Q]$ defines a linear operator on Q . Hence, we can rewrite (5.12) as

$$\begin{aligned} \frac{\partial Q}{\partial t} &= -\mu, \\ \mu &= \mathcal{L}Q + \frac{r(t)}{\sqrt{\mathcal{E}_1}} \frac{\delta\mathcal{E}_1}{\delta Q}[Q], \\ \frac{dr}{dt} &= \frac{1}{2\sqrt{\mathcal{E}_1}} \left(\frac{\delta\mathcal{E}_1}{\delta Q}[Q], \frac{\partial Q}{\partial t} \right). \end{aligned} \tag{5.15}$$

where we define the inner product as $(A, B) = \int_{\Omega} \sum_{i,j=1}^3 A_{ij}B_{ij}d\mathbf{x}$. Then the SAV/CN scheme for (5.15) is

$$\frac{Q^{n+1} - Q^n}{\Delta t} = -\mu^{n+1/2}, \tag{5.16a}$$

$$\mu^{n+1/2} = \mathcal{L} \frac{1}{2}(Q^{n+1} + Q^n) + \frac{r^{n+1} + r^n}{2\sqrt{\mathcal{E}_1[\bar{Q}^{n+1/2}]} } \frac{\delta\mathcal{E}_1}{\delta Q}[\bar{Q}^{n+1/2}], \tag{5.16b}$$

$$r^{n+1} - r^n = \frac{1}{2\sqrt{\mathcal{E}_1[\bar{Q}^{n+1/2}]} } \left(\frac{\delta\mathcal{E}_1}{\delta Q}[\bar{Q}^{n+1/2}], Q^{n+1} - Q^n \right). \tag{5.16c}$$

One can easily show that the above scheme is unconditionally energy stable. Below, we describe how to implement it efficiently.

Denoting

$$S = \frac{1}{2\sqrt{\mathcal{E}_1[\bar{Q}^{n+1/2}]} } \frac{\delta\mathcal{E}_1}{\delta Q}[\bar{Q}^{n+1/2}],$$

we can rewrite (5.16) as a coupled linear system of the form

$$(1 + \lambda\mathcal{L})Q^{n+1} + \frac{\lambda}{2}S(S, Q^{n+1}) = b^n, \quad 1 \leq i, j \leq 3, \tag{5.17}$$

where $\lambda = \frac{\Delta t}{2}$, and the scalar $\alpha^{n+1} = (S, Q^{n+1})$ can be solved explicitly as follows. Multiplying (5.17) with $(1 + \lambda\mathcal{L})^{-1}$, we find

$$Q^{n+1} + \frac{\lambda}{2} \cdot \alpha^{n+1}(I + \lambda\mathcal{L})^{-1}S = (1 + \lambda\mathcal{L})^{-1}b^n. \tag{5.18}$$

Taking the inner product of the above with S , we then obtain

$$\alpha^{n+1} \left(1 + \frac{\lambda}{2} (S, (1 + \lambda\mathcal{L})^{-1}S) \right) = (S, (I + \lambda\mathcal{L})^{-1}b^n). \tag{5.19}$$

Thus, we can find α^{n+1} by solving two equations of the form

$$(5.20) \quad (I + \lambda\mathcal{L})Q = g,$$

which can be efficiently solved since they are simply coupled second-order equations with constant coefficients. For example, in the case of periodic boundary conditions, we can write down the solution explicitly as follows. Because Q is symmetric and traceless, we choose $\mathbf{x} = (Q_{11}, Q_{22}, Q_{12}, Q_{13}, Q_{23})^T$ as independent variables. We expand the above five variables using Fourier series,

$$Q_{ij} = \sum_{k_1, k_2, k_3} \hat{Q}_{ij}^{k_1 k_2 k_3} \exp(i(k_1 x_1 + k_2 x_2 + k_3 x_3)).$$

Then, when solving the linear equation (5.20), only the Fourier coefficients with the same indices (k_1, k_2, k_3) are coupled. More precisely, for each (k_1, k_2, k_3) , the coefficient matrix for the unknowns $\hat{Q}_{ij}^{k_1 k_2 k_3}$ with $(ij = 11, 22, 12, 13, 23)$ is given by

$$A_{k_1 k_2 k_3} = 1 + \lambda(a_1 + L_1(k_1^2 + k_2^2 + k_3^2))I - \lambda(L_2 + L_3) \begin{pmatrix} -\frac{2}{3}k_1^2 - \frac{1}{3}k_3^2 & \frac{1}{3}k_2^2 - \frac{1}{3}k_3^2 & -\frac{1}{3}k_1 k_2 & -\frac{1}{3}k_1 k_3 & \frac{2}{3}k_2 k_3 \\ \frac{1}{3}k_1^2 - \frac{1}{3}k_3^2 & -\frac{2}{3}k_2^2 - \frac{1}{3}k_3^2 & -\frac{1}{3}k_1 k_2 & \frac{2}{3}k_1 k_3 & -\frac{1}{3}k_2 k_3 \\ -\frac{1}{2}k_1 k_2 & -\frac{1}{2}k_1 k_2 & -\frac{1}{2}k_1^2 - \frac{1}{2}k_2^2 & -\frac{1}{2}k_2 k_3 & -\frac{1}{2}k_1 k_3 \\ 0 & \frac{1}{2}k_1 k_3 & -\frac{1}{2}k_2 k_3 & -\frac{1}{2}k_1^2 - \frac{1}{2}k_3^2 & -\frac{1}{2}k_1 k_2 \\ \frac{1}{2}k_2 k_3 & 0 & -\frac{1}{2}k_1 k_3 & -\frac{1}{2}k_1 k_2 & -\frac{1}{2}k_2^2 - \frac{1}{2}k_3^2 \end{pmatrix}.$$

Hence, we can obtain the Fourier coefficients $\hat{Q}_{ij}^{k_1 k_2 k_3}$ for each i, j by inverting the above 5×5 matrix.

Example 8. We use SAV/CN to solve (5.12) in $[0, L]^2$, $L = 2\pi$, with periodic boundary conditions, discretized with 64×64 Fourier series and $\Delta t = 10^{-3}$. The parameters are chosen as $a = -1/25$, $b = c = 1$, $L_1 = L_2 + L_3 = 1$, and $a_1 = 0$, $C_0 = 10$.

With these parameters, the global minimizers of the bulk energy density $f_b(Q)$ can be written as

$$(5.21) \quad Q = \frac{3}{5}(\mathbf{n} \otimes \mathbf{n} - \frac{1}{3}I),$$

where \mathbf{n} is arbitrary unit vector. We choose the initial value such that $Q(x, y)$ has this form at each point, with

$$(5.22) \quad \mathbf{n}(x, y) = \begin{cases} (1, 0, 0)^T, & |x - \frac{L}{2}| \leq \frac{L}{4} \text{ and } |y - \frac{L}{2}| \leq \frac{L}{4}, \\ (0, 1, 0)^T, & |x - \frac{L}{2}| > \frac{L}{4} \text{ or } |y - \frac{L}{2}| > \frac{L}{4}. \end{cases}$$

To present the result, we draw the field of the principal eigenvector of $Q(x, y)$ (see Figure 11), representing the direction along which liquid crystalline molecules accumulate. Initially, the principal eigenvector is along the x -direction in a square region, while it is along the y -direction elsewhere. The square region is first driven into a circle by the gradient flow, then shrinks until it vanishes. The energy evolution, with the original and modified energies indistinguishable, is shown in Figure 12. We observe that the energy dissipation is satisfied.

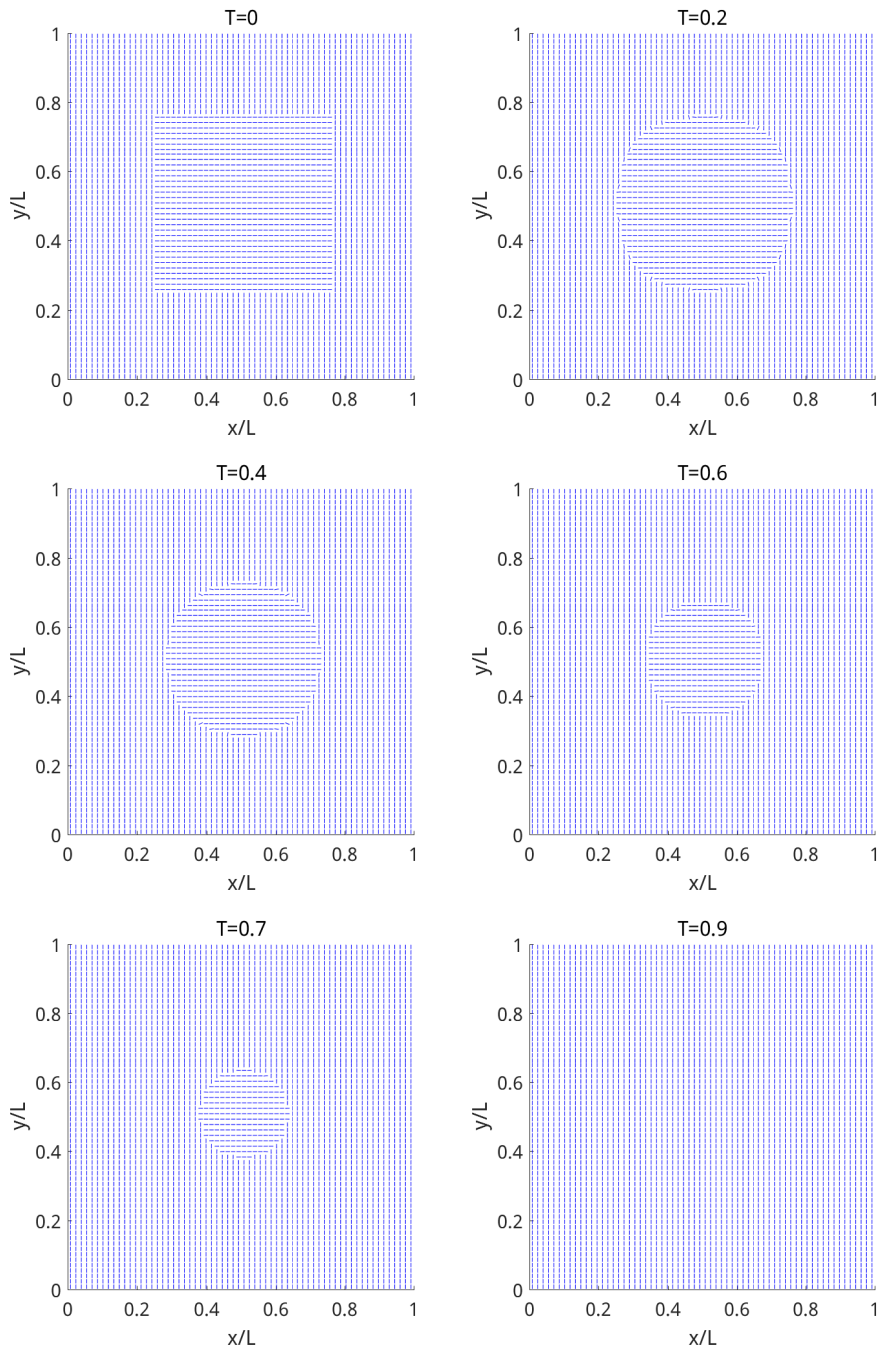


Fig. 11 (Example 8.) Evolution of the principal eigenvector.

6. Conclusion. We have proposed a new SAV approach for dealing with a large class of gradient flows. This approach keeps all the advantages of the IEQ approach, namely, the schemes are unconditionally stable about a modified energy and are linear and second-order accurate, while it offers the following additional advantages:

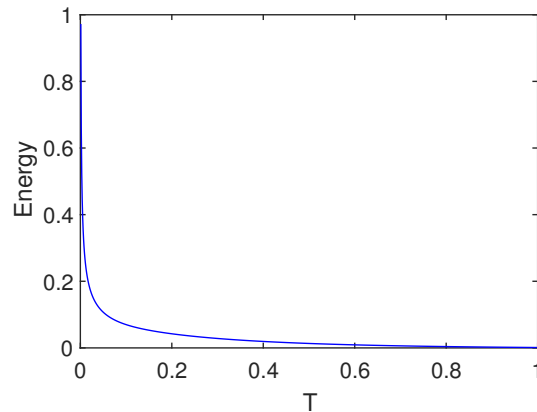


Fig. 12 (Example 8.) Energy evolution.

- It greatly simplifies the implementation and is much more efficient: at each time step of the SAV schemes, the computations of the SAV r^{m+1} and that of the original unknowns are totally decoupled and only require solving linear systems with constant coefficients.
- It only requires that $\mathcal{E}_1[\phi] = \int_{\Omega} g(\phi, \dots, \nabla^m \phi) d\mathbf{x}$, rather than $g(\phi, \dots, \nabla^m \phi)$, is bounded from below. It also allows us to deal with nonlinear energy functionals without the above form, for example, those containing multiple integrals. Thus, it applies to a larger class of gradient flows. In particular, it offers an effective approach to deal with gradient flows with nonlocal free energy.

Furthermore, we can even construct higher-order stiffly stable schemes with all the above attributes by combining the SAV approach with higher-order BDF schemes. Also, when coupled with a suitable time adaptive strategy, the SAV schemes are extremely efficient and applicable to a large class of gradient flows.

Although the SAV approach appears to be applicable for a large class of gradient flows, an essential requirement for it to produce physically consistent results is that \mathcal{L} in the energy splitting (1.3) contains sufficient dissipative terms (with at least linearized highest derivative terms) such that $\mathcal{E}_1[\phi]$ is not “dominant.” This can usually be achieved with a clever splitting of the free energy; (3.3) is such an example. A better splitting can lead to better accuracy. The splitting of energy relies on an understanding of the free energy and needs to be discussed case by case. Thus, it is a problem that requires further study.

We have focused in this paper on gradient flows with linear dissipative mechanisms. For problems with highly nonlinear dissipative mechanisms, e.g., $\mathcal{G}\mu = \nabla \cdot (a(\phi)\nabla\mu)$ with degenerate or singular $a(\phi)$, such as in Wasserstein gradient flows or gradient flows with strong anisotropic free energy [15], the direct application of the SAV approach may not be the most efficient as it leads to degenerate or singular nonlinear equations to solve at each time step. In [67], we developed an efficient predictor-corrector strategy to deal with this type of problem without the need to solve nonlinear equations.

There may also be obstacle potentials, such as logarithmic potentials, in the nonlinear free energy that impose constraints on the unknown functions. In some PDEs,

these constraints are also crucial for the dissipative operators to be nonpositive. The SAV approach does not provide a mechanism that keeps these constraints in the time-discretized schemes. To ensure that the numerical solutions satisfy these constraints, one may need to add restrictions on the time step or find alternative approaches.

While it is important that numerical schemes for gradient flows obey a discrete energy dissipation law, the energy dissipation itself does not guarantee the convergence. In another work [66], convergence and error analysis for the SAV approach is carried out. It is proved that with mild conditions on the nonlinear term \mathcal{E}_1 , the SAV schemes converge to the exact solution of the original problem at a rate identical to the truncation error. This applies to most of the equations discussed in this paper.

REFERENCES

- [1] M. AINSWORTH AND Z. MAO, *Analysis and approximation of a fractional Cahn–Hilliard equation*, SIAM J. Numer. Anal., 55 (2017), pp. 1689–1718, <https://doi.org/10.1137/16M1075302>. (Cited on pp. 475, 485, 488)
- [2] S. M. ALLEN AND J. W. CAHN, *A microscopic theory for antiphase boundary motion and its application to antiphase domain coarsening*, Acta Metallurgica, 27 (1979), pp. 1085–1095. (Cited on p. 485)
- [3] D. ANDELMAN, F. BROCHARD, AND J.-F. JOANNY, *Phase transitions in Langmuir monolayers of polar molecules*, J. Chem. Phys., 86 (1987), pp. 3673–3681. (Cited on p. 488)
- [4] D. M. ANDERSON, G. B. MCFADDEN, AND A. A. WHEELER, *Diffuse-interface methods in fluid mechanics*, Annu. Rev. Fluid Mech., 30 (1998), pp. 139–165. (Cited on pp. 475, 485)
- [5] A. J. ARCHER, A. RUCKLIDGE, AND E. KNOBLOCH, *Quasicrystalline order and a crystal-liquid state in a soft-core fluid*, Phys. Rev. Lett., 111 (2013), art. 165501. (Cited on p. 496)
- [6] S. BADIA, F. GUILLÉN-GONZÁLEZ, AND J. V. GUTIÉRREZ-SANTACREU, *Finite element approximation of nematic liquid crystal flows using a saddle-point structure*, J. Comput. Phys., 230 (2011), pp. 1686–1706. (Cited on p. 477)
- [7] K. BARKAN, M. ENGEL, AND R. LIFSHITZ, *Controlled self-assembly of periodic and aperiodic cluster crystals*, Phys. Rev. Lett., 113 (2014), art. 098304. (Cited on p. 496)
- [8] J. W. BARRETT AND J. F. BLOWEY, *Finite element approximation of a model for phase separation of a multi-component alloy with non-smooth free energy*, Numer. Math., 77 (1997), pp. 1–34. (Cited on pp. 476, 482)
- [9] J. W. BARRETT AND J. F. BLOWEY, *Finite element approximation of a model for phase separation of a multi-component alloy with a concentration-dependent mobility matrix*, IMA J. Numer. Anal., 18 (1998), pp. 287–328. (Cited on pp. 476, 482)
- [10] A. BASKARAN, J. S. LOWENGRUB, C. WANG, AND S. M. WISE, *Convergence analysis of a second order convex splitting scheme for the modified phase field crystal equation*, SIAM J. Numer. Anal., 51 (2013), pp. 2851–2873, <https://doi.org/10.1137/120880677>. (Cited on p. 476)
- [11] F. BOYER AND S. MINJEAUD, *Hierarchy of consistent n-component Cahn–Hilliard systems*, Math. Models Methods Appl. Sci., 24 (2014), pp. 2885–2928. (Cited on p. 482)
- [12] S. BRAZOVSKII, *Phase transition of an isotropic system to a nonuniform state*, Soviet JETP, 41 (1975), pp. 85–89. (Cited on p. 488)
- [13] J. W. CAHN AND J. E. HILLIARD, *Free energy of a nonuniform system. I. Interfacial free energy*, J. Chem. Phys., 28 (1958), pp. 258–267. (Cited on p. 485)
- [14] J. W. CAHN AND J. E. HILLIARD, *Free energy of a nonuniform system. III. Nucleation in a two-component incompressible fluid*, J. Chem. Phys., 31 (1959), pp. 688–699. (Cited on p. 485)
- [15] F. CHEN AND J. SHEN, *Efficient energy stable schemes with spectral discretization in space for anisotropic Cahn–Hilliard systems*, Commun. Comput. Phys., 13 (2013), pp. 1189–1208. (Cited on p. 502)
- [16] L. CHEN, *Phase-field models for microstructure evolution*, Annu. Rev. Mat. Res., 32 (2002), pp. 113–140. (Cited on p. 482)
- [17] L. Q. CHEN AND J. SHEN, *Applications of semi-implicit Fourier-spectral method to phase field equations*, Comput. Phys. Commun., 108 (1998), pp. 147–158. (Cited on p. 486)
- [18] W. CHEN, S. CONDE, C. WANG, X. WANG, AND S. WISE, *A linear energy stable scheme for a thin film model without slope selection*, J. Sci. Comput., 52 (2012), pp. 546–562. (Cited on p. 497)

- [19] M. CHENG AND J. A. WARREN, *An efficient algorithm for solving the phase field crystal model*, J. Comput. Phys., 227 (2008), pp. 6241–6248. (Cited on p. 490)
- [20] Q. CHENG, J. SHEN, AND X. YANG, *Highly efficient and accurate numerical schemes for the epitaxial thin film growth models by using the SAV approach*, J. Sci. Comput., 78 (2019), pp. 1467–1487, <https://doi.org/10.1007/s10915-018-0832-5>. (Cited on pp. 497, 498)
- [21] S. M. COX AND P. C. MATTHEWS, *Exponential time differencing for stiff systems*, J. Comput. Phys., 176 (2002), pp. 430–455. (Cited on p. 486)
- [22] P. DE GENNES, *Short range order effects in the isotropic phase of nematics and cholesterics*, Molecular Crystals Liquid Crystals, 12 (1971), pp. 193–214. (Cited on p. 498)
- [23] M. DOI AND S. F. EDWARDS, *The Theory of Polymer Dynamics*, Oxford University Press, 1988. (Cited on p. 475)
- [24] S. DONG, *An efficient algorithm for incompressible N -phase flows*, J. Comput. Phys., 276 (2014), pp. 691–728. (Cited on p. 482)
- [25] Q. DU AND J. YANG, *Fast and accurate implementation of Fourier spectral approximations of nonlocal diffusion operators and its applications*, J. Comput. Phys., 332 (2017), pp. 118–134. (Cited on p. 490)
- [26] K. ELDER AND M. GRANT, *Modeling elastic and plastic deformations in nonequilibrium processing using phase field crystals*, Phys. Rev. E, 70 (2004), art. 051605. (Cited on pp. 475, 489)
- [27] K. ELDER, M. KATAKOWSKI, M. HAATAJA, AND M. GRANT, *Modeling elasticity in crystal growth*, Phys. Rev. Lett., 88 (2002), art. 245701. (Cited on pp. 475, 489)
- [28] K. ELDER, N. PROVATAS, J. BERRY, P. STEFANOVIC, AND M. GRANT, *Phase-field crystal modeling and classical density functional theory of freezing*, Phys. Rev. B, 75 (2007), art. 064107. (Cited on pp. 475, 489)
- [29] C. M. ELLIOTT AND A. M. STUART, *The global dynamics of discrete semilinear parabolic equations*, SIAM J. Numer. Anal., 30 (1993), pp. 1622–1663, <https://doi.org/10.1137/0730084> (Cited on p. 476)
- [30] D. J. EYRE, *Systems of Cahn–Hilliard equations*, SIAM J. Appl. Math., 53 (1993), pp. 1686–1712, <https://doi.org/10.1137/0153078>. (Cited on p. 482)
- [31] D. J. EYRE, *Unconditionally gradient stable time marching the Cahn–Hilliard equation*, in MRS Proc. 529, Cambridge University Press, 1998, p. 39. (Cited on p. 476)
- [32] M. G. FOREST, Q. WANG, AND R. ZHOU, *The flow-phase diagram of Doi-Hess theory for sheared nematic polymers II: Finite shear rates*, Rheologica Acta, 44 (2004), pp. 80–93. (Cited on p. 475)
- [33] M. G. FOREST, Q. WANG, AND R. ZHOU, *The weak shear kinetic phase diagram for nematic polymers*, Rheologica Acta, 43 (2004), pp. 17–37. (Cited on p. 475)
- [34] J. FRAAIE, *Dynamic density functional theory for microphase separation kinetics of block copolymer melts*, J. Chem. Phys., 99 (1993), pp. 9202–9212. (Cited on p. 475)
- [35] J. FRAAIE AND G. SEVINK, *Model for pattern formation in polymer surfactant nanodroplets*, Macromolecules, 36 (2003), pp. 7891–7893. (Cited on p. 475)
- [36] J. FRAAIE, B. VAN VLIMMEREN, N. MAURITS, M. POSTMA, O. EVERS, C. HOFFMANN, P. ALTEVOGT, AND G. GOLDBECK-WOOD, *The dynamic mean-field density functional method and its application to the mesoscopic dynamics of quenched block copolymer melts*, J. Chem. Phys., 106 (1997), pp. 4260–4269. (Cited on p. 475)
- [37] T. GAREL AND S. DONIACH, *Phase transitions with spontaneous modulation—the dipolar Ising ferromagnet*, Phys. Rev. B, 26 (1982), pp. 325–329. (Cited on p. 488)
- [38] L. GIACOMELLI AND F. OTTO, *Variational formulation for the lubrication approximation of the Hele-Shaw flow*, Calc. Var. Partial Differential Equations, 13 (2001), pp. 377–403. (Cited on p. 475)
- [39] G. H. GOLUB AND C. F. VAN LOAN, *Matrix Computations*, 4th ed., Johns Hopkins Studies in the Mathematical Sciences, Johns Hopkins University Press, Baltimore, MD, 2013. (Cited on p. 484)
- [40] G. GOMPPER AND M. SCHICK, *Correlation between structural and interfacial properties of amphiphilic systems*, Phys. Rev. Lett., 65 (1990), pp. 1116–1119. (Cited on p. 488)
- [41] F. GUILLÉN-GONZÁLEZ AND G. TIERRA, *On linear schemes for a Cahn–Hilliard diffuse interface model*, J. Comput. Phys., 234 (2013), pp. 140–171. (Cited on p. 477)
- [42] M. E. GURTIN, D. POLIGNONE, AND J. VINALS, *Two-phase binary fluids and immiscible fluids described by an order parameter*, Math. Models Methods Appl. Sci., 6 (1996), pp. 815–831. (Cited on pp. 475, 485)
- [43] K. JIANG, P. ZHANG, AND A.-C. SHI, *Stability of icosahedral quasicrystals in a simple model with two-length scales*, J. Phys. Condensed Matter, 29 (2017), art. 124003. (Cited on p. 496)

- [44] R. JORDAN, D. KINDERLEHRER, AND F. OTTO, *The variational formulation of the Fokker–Planck equation*, SIAM J. Math. Anal., 29 (1998), pp. 1–17, <https://doi.org/10.1137/S0036141096303359>. (Cited on p. 475)
- [45] L. JU, J. ZHANG, L. ZHU, AND Q. DU, *Fast explicit integration factor methods for semilinear parabolic equations*, J. Sci. Comput., 62 (2015), pp. 431–455. (Cited on p. 477)
- [46] J. KIM, *Phase-field models for multi-component fluid flows*, Commun. Comput. Phys., 12 (2012), pp. 613–661. (Cited on pp. 475, 485)
- [47] R. LARSON, *Arrested tumbling in shearing flows of liquid crystal polymers*, Macromolecules, 23 (1990), pp. 3983–3992. (Cited on p. 475)
- [48] R. LARSON AND H. ÖTTINGER, *Effect of molecular elasticity on out-of-plane orientations in shearing flows of liquid-crystalline polymers*, Macromolecules, 24 (1991), pp. 6270–6282. (Cited on p. 475)
- [49] F. LESLIE, *Theory of flow phenomena in liquid crystals*, Adv. Liquid Crystals, 4 (1979), pp. 1–81. (Cited on p. 475)
- [50] B. LI AND J.-G. LIU, *Thin film epitaxy with or without slope selection*, European J. Appl. Math., 14 (2003), pp. 713–743. (Cited on pp. 497, 498)
- [51] D. LI AND Z. QIAO, *On second order semi-implicit Fourier spectral methods for 2D Cahn–Hilliard equations*, J. Sci. Comput., 70 (2017), pp. 301–341. (Cited on p. 477)
- [52] C. LIU AND J. SHEN, *A phase field model for the mixture of two incompressible fluids and its approximation by a Fourier-spectral method*, Phys. D, 179 (2003), pp. 211–228. (Cited on pp. 475, 485)
- [53] J. LOWENGRUB AND L. TRUSKINOVSKY, *Quasi-incompressible Cahn–Hilliard fluids and topological transitions*, R. Soc. Lond. Proc. Ser. A Math. Phys. Eng. Sci., 454 (1998), pp. 2617–2654. (Cited on pp. 475, 485)
- [54] J. F. LUTSKO, *Recent developments in classical density functional theory*, Adv. Chem. Phys., 144 (2010), pp. 1–9. (Cited on p. 496)
- [55] A. MAJUMDAR, *The radial-hedgehog solution in Landau–de Gennes’ theory for nematic liquid crystals*, European J. Appl. Math., 23 (2012), pp. 61–97. (Cited on p. 498)
- [56] N. MAURITS AND J. FRAAIJE, *Mesoscopic dynamics of copolymer melts: From density dynamics to external potential dynamics using nonlocal kinetic coupling*, J. Chem. Phys., 107 (1997), pp. 5879–5889. (Cited on p. 475)
- [57] R. NÜRNBERG, *Numerical simulations of immiscible fluid clusters*, Appl. Numer. Math., 59 (2009), pp. 1612–1628. (Cited on p. 482)
- [58] F. OTTO, *Lubrication approximation with prescribed nonzero contact angle*, Comm. Partial Differential Equations, 23 (1998), pp. 2077–2164. (Cited on p. 475)
- [59] M. PAICU AND A. ZARNESCU, *Energy dissipation and regularity for a coupled Navier–Stokes and Q -tensor system*, Arch. Ration. Mech. Anal., 203 (2012), pp. 45–67. (Cited on p. 498)
- [60] T. QIAN AND P. SHENG, *Generalized hydrodynamic equations for nematic liquid crystals*, Phys. Rev. E, 58 (1998), pp. 7475–7485. (Cited on p. 475)
- [61] Z. QIAO, Z.-Z. SUN, AND Z. ZHANG, *Stability and convergence of second-order schemes for the nonlinear epitaxial growth model without slope selection*, Math. Comp., 84 (2015), pp. 653–674. (Cited on p. 498)
- [62] T. ROGERS AND R. C. DESAI, *Numerical study of late-stage coarsening for off-critical quenches in the Cahn–Hilliard equation of phase separation*, Phys. Rev. B, 39 (1989), pp. 11956–11964. (Cited on p. 485)
- [63] N. SCHOPHIL AND T. SLUCKIN, *Defect core structure in nematic liquid crystals*, Phys. Rev. Lett., 59 (1987), pp. 2582–2584. (Cited on p. 498)
- [64] J. SHEN, T. TANG, AND J. YANG, *On the maximum principle preserving schemes for the generalized Allen–Cahn equation*, Comm. Math. Sci., 14 (2016), pp. 1517–1534. (Cited on p. 494)
- [65] J. SHEN, C. WANG, X. WANG, AND S. M. WISE, *Second-order convex splitting schemes for gradient flows with Ehrlich–Schwoebel type energy: Application to thin film epitaxy*, SIAM J. Numer. Anal., 50 (2012), pp. 105–125, <https://doi.org/10.1137/110822839>. (Cited on pp. 476, 498)
- [66] J. SHEN AND J. XU, *Convergence and error analysis for the scalar auxiliary variable (SAV) schemes to gradient flows*, SIAM J. Numer. Anal., 56 (2018), pp. 2895–2912, <https://doi.org/10.1137/17M1159968>. (Cited on p. 503)
- [67] J. SHEN AND J. XU, *Stabilized predictor-corrector schemes for gradient flows with strong anisotropic free energy*, Commun. Comput. Phys., 24 (2018), pp. 635–654. (Cited on p. 502)
- [68] J. SHEN, J. XU, AND J. YANG, *The scalar auxiliary variable (SAV) approach for gradient flows*, J. Comput. Phys., 353 (2018), pp. 407–416. (Cited on pp. 478, 482)

- [69] J. SHEN AND X. YANG, *Numerical approximations of Allen-Cahn and Cahn-Hilliard equations*, *Discrete Contin. Dyn. Syst.*, 28 (2010), pp. 1669–1691. (Cited on pp. 476, 485, 487)
- [70] P. SHENG, *Boundary-layer phase transition in nematic liquid crystals*, *Phys. Rev. A*, 26 (1982), pp. 1610–1617. (Cited on p. 498)
- [71] S. A. SILLING, *Reformulation of elasticity theory for discontinuities and long-range forces*, *J. Mech. Phys. Solids*, 48 (2000), pp. 175–209. (Cited on pp. 489, 496)
- [72] X. WU, G. J. VAN ZWIETEN, AND K. G. VAN DER ZEE, *Stabilized second-order convex splitting schemes for Cahn-Hilliard models with application to diffuse-interface tumor-growth models*, *Int. J. Numer. Methods Biomed. Eng.*, 30 (2014), pp. 180–203. (Cited on p. 476)
- [73] J. XU, C. WANG, A.-C. SHI, AND P. ZHANG, *Computing optimal interfacial structure of modulated phases*, *Commun. Comput. Phys.*, 21 (2017), pp. 1–15. (Cited on p. 488)
- [74] X. YANG, *Linear, first and second-order, unconditionally energy stable numerical schemes for the phase field model of homopolymer blends*, *J. Comput. Phys.*, 327 (2016), pp. 294–316. (Cited on p. 477)
- [75] H. YU, G. JI, AND P. ZHANG, *A nonhomogeneous kinetic model of liquid crystal polymers and its thermodynamic closure approximation*, *Commun. Comput. Phys.*, 7 (2010), p. 383. (Cited on p. 475)
- [76] P. YUE, J. J. FENG, C. LIU, AND J. SHEN, *A diffuse-interface method for simulating two-phase flows of complex fluids*, *J. Fluid Mech.*, 515 (2004), pp. 293–317. (Cited on pp. 475, 485)
- [77] J. ZHAO, Q. WANG, AND X. YANG, *Numerical approximations for a phase field dendritic crystal growth model based on the invariant energy quadratization approach*, *Internat. J. Numer. Methods Engrg.*, 110 (2017), pp. 279–300. (Cited on p. 477)
- [78] J. ZHAO, X. YANG, Y. GONG, AND Q. WANG, *A novel linear second order unconditionally energy stable scheme for a hydrodynamic-tensor model of liquid crystals*, *Comput. Methods Appl. Mech. Engrg.*, 318 (2017), pp. 803–825. (Cited on p. 498)
- [79] J. ZHU, L. CHEN, J. SHEN, AND V. TIKARE, *Coarsening kinetics from a variable mobility Cahn-Hilliard equation—application of semi-implicit Fourier spectral method*, *Phys. Rev. E.*, 60 (1999), pp. 3564–3572. (Cited on p. 476)